Department of Radio Science and Engineering

Magnetic materials and responses in antenna applications

Antti Karilainen

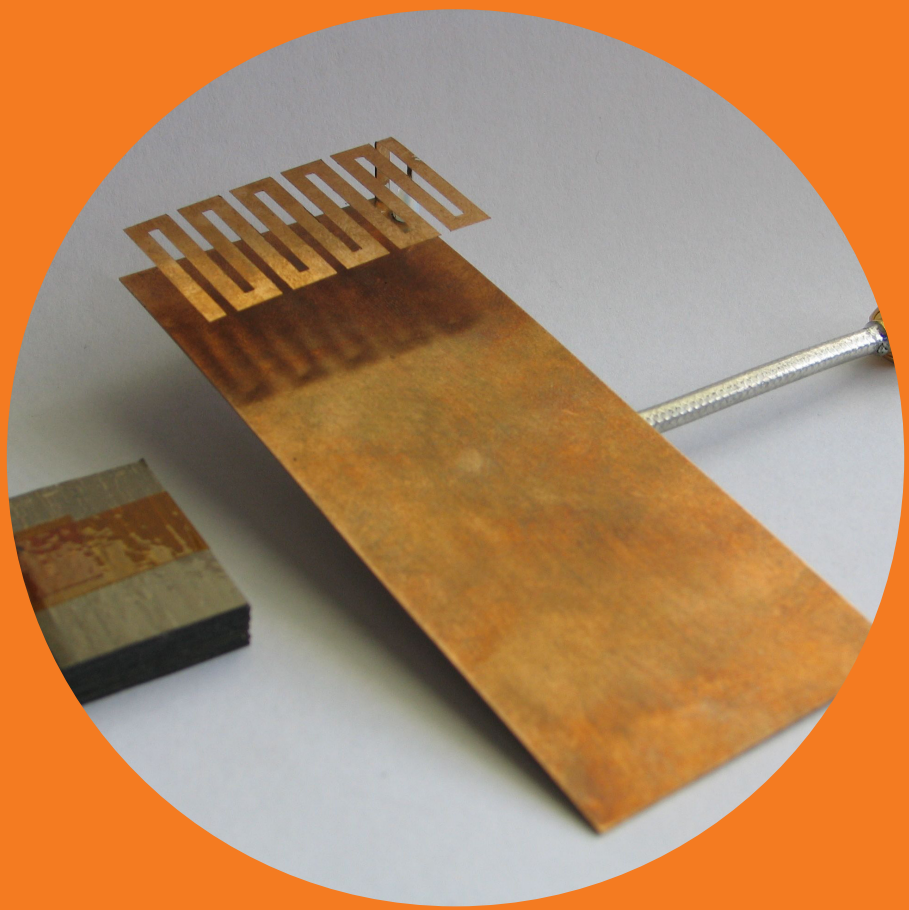

Aalto University

DOCTORAL DISSERTATIONS

Aalto University publication series
DOCTORAL DISSERTATIONS 93/2012

Magnetic materials and responses in antenna applications

Antti Karilainen

Doctoral dissertation for the degree of Doctor of Science in Technology to be presented with due permission of the School of Electrical Engineering for public examination and debate in Auditorium S1 at the Aalto University School of Electrical Engineering (Otakaari 5 A, Espoo, Finland) on the 10th of August 2012 at 12 o'clock noon.

Aalto University
School of Electrical Engineering
Department of Radio Science and Engineering

Supervising professor
Prof. Sergei Tretyakov

Thesis advisor
Prof. Sergei Tretyakov

Preliminary examiners
Prof. Andrea Alù, University of Texas at Austin, Austin, TX, USA
Prof. Ferran Martin, Universitat Autònoma de Barcelona, Barcelona, Spain

Opponent
Prof. Richard Ziolkowski, University of Arizona, Tucson, AZ, USA

Aalto University publication series
DOCTORAL DISSERTATIONS 93/2012

ISBN 978-952-60-4704-1 (printed)
ISBN 978-952-60-4705-8 (pdf)
ISSN-L 1799-4934
ISSN 1799-4934 (printed)
ISSN 1799-4942 (pdf)
http://urn.fi/URN:ISBN:978-952-60-4705-8

Unigrafia Oy
Helsinki 2012

Finland

441 697
Printed matter

Aalto University

Abstract

Aalto University, P.O. Box 11000, FI-00076 Aalto www.aalto.fi

Author
Antti Karilainen

Name of the doctoral dissertation
Magnetic materials and responses in antenna applications

Publisher School of Electrical Engineering

Unit Department of Radio Science and Engineering

Series Aalto University publication series DOCTORAL DISSERTATIONS 93/2012

Field of research Radio Engineering

Manuscript submitted 5 March 2012 **Date of the defence** 10 August 2012

Permission to publish granted (date) 15 May 2012 **Language** English

☐ **Monograph** ☒ **Article dissertation (summary + original articles)**

Abstract

Electric and magnetic fields have been known to be a manifestation of the same physical phenomenon for almost two hundred years, but some aspects of electromagnetism are not in balance in nature around us. We are faced with restrictions due to lack of real magnetic charges, currents, and conductors. However, it has turned out that virtual magnetic currents and conductors and magnetic materials can be engineered and used in a variety of applications, antennas being one amongst them.

This doctoral thesis focuses on magnetic materials and artificially created magnetic responses in antenna applications. The thesis is divided into three parts concerning antennas in which the magnetic part of Maxwell's equations plays a key role. The common goal in each of these parts is to improve the properties of the antennas in question or to conjure new types of antennas.

The first part of the thesis deals with antenna miniaturisation using magnetic materials. A new method to determine the optimal material for a given small resonant antenna is proposed. The method is based on identifying the radiating field (equivalent current) of the antenna. A mobile-terminal antenna is miniaturised with dielectric and magneto-dielectric (both dielectric and magnetic responses) materials. Guidelines for an objective comparison of filling materials in antenna miniaturisation are presented.

In the second part the antenna in question is based on a mushroom type high-impedance surface (HIS). The modes of an HIS are studied by using an analytical model for oblique incidence angles of the incident plane wave. Two of the resonance modes responsible for the HIS behaviour in the infinitely-sized surface are identified and used as a basis for designing a finite antenna with two orthogonal radiation patterns.

A helical antenna geometry based on wires and loops is studied in the third part. By using a combination of short electric dipoles and loops acting as magnetic elementary dipoles, a Huygens' source antenna for circular polarisation (CP) from two helices is designed. Huygens' source antenna has a unidirectional radiation pattern and perfect polarisation purity: In theory it can radiate perfect CP in every direction, making it, for example, an attractive receiving antenna for space-to-Earth communications. The geometry of the antenna has also a peculiar effect when an incoming wave is scattered from the object, as the scattered field is directed away from the object when the incoming field arrives from certain directions.

Keywords antennas, magnetic material, mobile antennas, high-impedance surface, receiving antennas, scattering

ISBN (printed) 978-952-60-4704-1 **ISBN (pdf)** 978-952-60-4705-8

ISSN-L 1799-4934 **ISSN (printed)** 1799-4934 **ISSN (pdf)** 1799-4942

Location of publisher Espoo **Location of printing** Helsinki **Year** 2012

Pages 114 **urn** http://urn.fi/URN:ISBN:978-952-60-4705-8

Tekijä
Antti Karilainen

Väitöskirjan nimi
Magneettiset materiaalit ja vasteet antennisovelluksissa

Julkaisija Sähkötekniikan korkeakoulu

Yksikkö Radiotieteen ja -tekniikan laitos

Sarja Aalto University publication series DOCTORAL DISSERTATIONS 93/2012

Tutkimusala Radiotekniikka

Käsikirjoituksen pvm 05.03.2012 **Väitöspäivä** 10.08.2012

Julkaisuluvan myöntämispäivä 15.05.2012 **Kieli** Englanti

☐ **Monografia** ☒ **Yhdistelmäväitöskirja (yhteenveto-osa + erillisartikkelit)**

Tiivistelmä

Sähkö- ja magneettikentän on tiedetty olevan saman fysikaalisen ilmentymän osia jo kohta kahdensadan vuoden ajan, mutta sähkömagnetismin jotkut puolet eivät ole tasapainossa ympärillämme luonnossa, sillä magneettisten varausten, virtojen ja johteiden puute aiheuttaa rajoituksia tietyissä sovelluksissa. Näennäisiä magneettisia virtoja ja johteita ja magneettisia materiaaleja voidaan tuottaa keinotekoisesti ja käyttää monissa sovelluksissa, joista yksi on antennit.

Tämä väitöskirja käsittelee magneettisia materiaaleja ja keinotekoisesti luotuja magneettisia vasteita antennisovelluksissa. Väitöskirja on jaettu kolmeen antenneja käsittelevään osaan, joissa Maxwellin yhtälöiden magneettinen puoli on avainroolissa. Yhteinen päämäärä näissä jokaisessa osassa on parantaa käsiteltävän antennin ominaisuuksia tai kehittää uudentyyppisiä antenneja.

Ensimmäinen osa käsittelee antennien miniatyrisointia magneettisia materiaaleja käyttäen. Uutta menetelmää ehdotetaan selvittämään optimaalinen materiaali pienelle resonoivalle antennille. Tämä menetelmä perustuu antennin säteilevän kentän eli ekvivalenttisen pintavirran tunnistamiseen. Matkapuhelinantennin miniatyrisointia testataan dielektrisellä sekä magnetodielektrisellä (sekä dielektrinen että magneettinen vaste) materiaaleilla. Materiaalien objektiiviseen vertailuun esitetään suosituksia.

Toisessa osassa kyseessä oleva antenni perustuu korkeaimpedanssipintaan, jonka moodeja tutkitaan käyttämällä tasoaallon epäsuorille tulokulmille kehitettyä analyyttistä mallia. Kaksi impedanssipinnan toiminnan kannalta olennaista resonanssimoodia tunnistetaan, ja niitä käytetään perustana äärellisen kokoiselle antennille, joka säteilee kahdella ortogonaalisella säteilykuviolla.

Kolmannessa osassa tutkitaan suoriin metallilankoihin ja silmukoihin perustuvaa spiraaliantennia. Kahdesta spiraalista muodostetaan ympyräpolarisoitu Huygensinlähdeantenni yhdistämällä lyhyitä sähködipoleita ja pieniä silmukoita, magneettidipoleita. Huygensinlähdeantennilla on yksisuuntainen säteilykuvio sekä täydellinen polarisaatiopuhtaus, sillä teoriassa se säteilee ympyräpolarisaatiota joka suuntaan ollen näin kiinnostava vastaanottoantenni esimerkiksi satelliittitietoliikennettä varten. Antennin muoto aiheuttaa myös mielenkiintoisen ilmiön siitä sironneeseen tasoaaltoon: sironnut kenttä suuntautuu pois aallon tulosuunnasta tietyillä tulokulmilla.

Avainsanat antennit, magneettiset materiaalit, mobiiliantennit, korkeaimpedanssipinta, vastaanottoantenni, sironta

ISBN (painettu) 978-952-60-4704-1 **ISBN (pdf)** 978-952-60-4705-8

ISSN-L 1799-4934 **ISSN (painettu)** 1799-4934 **ISSN (pdf)** 1799-4942

Julkaisupaikka Espoo **Painopaikka** Helsinki **Vuosi** 2012

Sivumäärä 114 **urn** http://urn.fi/URN:ISBN:978-952-60-4705-8

Preface

This doctoral thesis is a product of my work during a few years at the Department of Radio Science and Engineering at Aalto University School of Electrical Engineering. My warmest thanks go to my supervisor Prof. Sergei Tretyakov for hiring me to a job which I already once declined. Your Friday seminars were an inspiration to sometimes monotonous research work. I would also like to thank Prof. Constantin Simovski: your input to the seminars with Igor Nefedov was invaluable.

I hold in great value the help and cooperation of my co-authors Constantin Simovski, Pekka Alitalo, Olli Luukkonen, Pekka Ikonen, Joni Vehmas, Teemu Niemi, and Konstantin Rozanov and other authors at ITAE. It was a real pleasure to be able to work in different research projects with so many fellow researchers!

This thesis would have not been started without the excellent teaching in the undergraduate level provided by the department's professors Martti Valtonen, Ari Sihvola, Antti Räisänen, Keijo Nikoskinen, and other staff. Further, I would like to thank my high-school mathematics and physics teacher Esa Pärnänen, who got us interested in the University to begin with.

Writing a doctoral thesis can be a tedious job. My special thanks belong to my colleagues Pekka and Olli and also to Tero, Jari, Krista, Risto, Mikko, Veli-Matti, Katsu, Aki, Aleksi, Juho, Maria, Liisi, and Dmitry, just to name a few. Thank you for providing a relaxing and entertaining company during office hours and otherwise. Additional thanks belong to Aalto-yliopiston Sähköinsinöörikilta ry, especially the candy machine, and to our communal coffee brewer.

Thanks to the pre-examiner, Prof. Andrea Alù and Prof. Ferran Martin, for their encouraging feedback and comments.

The projects included in this thesis were supported by the Academy of Finland through the Centre-of-Excellence program with Nokia, Intel, and Euro-

pean Space Agency. Financial support for the author was provided by the Aalto University School of Electrical Engineering graduate school, Jenny and Antti Wihuri Foundation, HPY Research Foundation, Elektroniikkainsinöörien säätiö, and Nokia Foundation.

Infinite thanks go to my friends, some of which I have had the pleasure to know all the way from the second grade.

I would like to thank my parents Aulikki and Tapio for all kinds of support during the years.

Deepest thanks to Nina, my fellow cyclist and long-lost companion whom I finally found.

Helsinki, July 6, 2012,

Antti Karilainen

Contents

List of publications

This thesis consists of an overview and of the following publications which are referred to in the text by their Roman numerals.

I A. O. Karilainen, P. M. T. Ikonen, C. R. Simovski, and S. A. Tretyakov, "Choosing dielectric or magnetic material to optimize the bandwidth of miniaturized resonant antennas," *IEEE Transactions on Antennas and Propagation*, vol. 59, no. 11, pp. 3991–3998, November 2011.

II A. O. Karilainen, P. M. T. Ikonen, C. R. Simovski, S. A. Tretyakov, A. N. Lagarkov, S. A. Maklakov, K. N. Rozanov, and S. N. Starostenko, "Experimental studies of antenna miniaturisation using magneto-dielectric and dielectric materials," *IET Microwaves, Antennas and Propagation*, vol. 5, no. 4, pp. 495–502, April 2011.

III A. O. Karilainen, J. Vehmas, O. Luukkonen, and S. A. Tretyakov, "High-impedance-surface-based antenna with two orthogonal radiating modes," *IEEE Antennas and Wireless Propagation Letters*, vol 10, pp. 247–250, 2011.

IV P. Alitalo, A. O. Karilainen, T. Niemi, C. R. Simovski, and S. A. Tretyakov, "Design and realisation of an electrically small Huygens source for circular polarisation," *IET Microwaves, Antennas and Propagation*, vol. 5, pp. 783–789, May 2011.

V A. O. Karilainen and S. A. Tretyakov, "Circularly polarized receiving antenna incorporating two helices to achieve low backscattering," *IEEE Transactions on Antennas and Propagation*, vol. 60, no. 7, pp. 3471–3475, July 2012.

Author's contribution

Publication I: "Choosing dielectric or magnetic material to optimize the bandwidth of miniaturized resonant antennas"

The author had the main idea and responsibility for writing the publication. C. Simovski derived the analytical model in Section 4 C. P. Ikonen, C. Simovski, and S. Tretyakov supervised the work.

Publication II: "Experimental studies of antenna miniaturisation using magneto-dielectric and dielectric materials"

The author conducted the measurements, analysed the results, and had the main responsibility for writing the publication. The magneto-dielectric material was manufactured and Section 3 written by the authors from ITAE. P. Ikonen, C. Simovski, and S. Tretyakov supervised the work at Aalto.

Publication III: "High-impedance-surface-based antenna with two orthogonal radiating modes"

The author had the main responsibility for writing the publication. The simulations and the experimental parts were conducted by J. Vehmas and the author. The publication is based on earlier work by the authors and was supervised by O. Luukkonen and S. Tretyakov.

Publication IV: “Design and realisation of an electrically small Huygens source for circular polarisation”

The author produced Sections 2 and 3 and had the responsibility for writing the publication with P. Alitalo. P. Alitalo and T. Niemi conducted the simulations. T. Niemi conducted the measurements with the help of the author. The idea came from S. Tretyakov and C. Simovski who also supervised the work.

Publication V: “Circularly polarized receiving antenna incorporating two helices to achieve low backscattering”

The author had the main idea and responsibility for writing the publication. S. Tretyakov supervised the work.

List of abbreviations

HIS	high-impedance surface
LH	left hand
LHCP	left-hand circular polarisation
PEC	perfect electric conductor
PMC	perfect magnetic conductor
RH	right hand
RHCP	right-hand circular polarisation
TE	transverse electric field
TM	transverse magnetic field

List of symbols

a	radius of sphere/circle, period [m]
$\mathbf{B}$	magnetic flux density [As/m^2]
B	relative bandwidth
C	capacitance [F]
$\mathbf{D}$	electric flux density [Vs/m^2]
D	directivity of antenna
d	distance, thickness [m]
$\mathbf{E}$	electric field strength [V/m]
$\mathbf{F}$	radiation/scattering pattern
f	frequency [1/s]
$\mathbf{H}$	magnetic field strength [A/m]
$\mathbf{h}$	vector effective length [m]
$\overline{\overline{I}}$	unit dyadic
$\overline{\overline{I}}_\mathrm{t}$	transverse unit dyadic
I	complex current [A]
$\mathbf{J}$	electric current density [A/m^2]
$\mathbf{J}_\mathrm{s}$	electric surface current [A/m]
j	imaginary unit
k	wave number [1/m]
L	inductance [H]
l	length [m]
$\mathbf{M}$	magnetic current density [V/m^2]
$\mathbf{M}_\mathrm{s}$	magnetic surface current [V/m]
$\mathbf{m}$	magnetic dipole moment [Vms]
$\mathbf{n}$	surface-normal unit vector

P	power [W]
$\mathbf{p}$	electric dipole moment [Ams]
Q	quality factor
R	resistance [Ω]
$\mathbf{r}$	position vector of a field point
r	radial coordinate [m]
S	area of loop [m^2]
$\mathbf{u}$	direction unit vector
W	energy [J]
X	reactance [Ω]
Z	impedance [Ω]
$\overline{\overline{\alpha}}$	polarisability dyadic [varies]
β	damping factor
Γ	loss factor [rad/s]
ϵ	permittivity [As/Vm]
ϵ_0	vacuum permittivity [As/Vm]
ϵ_r	relative permittivity
$\overline{\overline{\zeta}}$	magnetoelectric dyadic [As/Vm]
η_0	free-space wave impedance [Ω]
η_r	radiation efficiency
θ	inclination coordinate
Λ	amplitude factor
λ	wavelength [m]
μ	permeability [Vs/Am]
μ_0	vacuum permeability [Vs/Am]
μ_r	relative permeability
$\overline{\overline{\xi}}$	magnetoelectric dyadic [Vs/Am]
ξ	phase shift [rad]
ρ	reflection coefficient
ϱ	electric volume charge density [As/m^3]
σ	electric conductivity [S/m] / scattering cross section [m^2]
ϕ	azimuth coordinate
ω	angular frequency [rad/s]

1. Introduction

Electric and magnetic fields have been known to be a manifestation of the same physical phenomenon for almost two hundred years, but some aspects of electromagnetism are not in balance in nature around us. We are faced with restrictions due to lack of real magnetic charges, currents, and conductors. Magnetic currents are available as so-called equivalent currents only when created with electric fields or currents. For the same reason magnetic conductors in the same sense as electrical conductors are not available. However, it has turned out that virtual magnetic currents and conductors can be engineered and used in a variety of applications, antennas being one amongst them.

Natural materials have also quite different electromagnetic responses, described with electric permittivity and magnetic permeability. Materials with permittivity above unity and low losses used, for example, as microwave insulators and substrates are available, but such materials with corresponding magnetic properties at wide range of frequencies are not readily available in nature. Like the magnetic currents and conductors, this kind of material response has to be mimicked or special materials have to be manufactured to achieve the desired magnetic effects.

This doctoral thesis focuses on magnetic materials and artificially created magnetic responses and currents in antenna applications. The thesis is divided into three research problems concerning antennas in which the magnetic part of Maxwell's equations plays a key role. The common goal in each of these problems is to improve the properties of the antennas in question or to conjure new types of antennas. The methodology used in studying the problems is based on analytical or semi-analytical modelling. These simple electromagnetic models are later validated by full-wave simulations of Maxwell's equations, measurements, or by both, if possible.

Analysis is based on time-harmonic Maxwell's equations at the angular fre-

quency ω using the $\exp(j\omega t)$ time convention, and they read [1]

$$\nabla \times \mathbf{E} = -j\omega\mathbf{B} - \mathbf{M}, \tag{1.1}$$

$$\nabla \times \mathbf{H} = j\omega\mathbf{D} + \mathbf{J}, \tag{1.2}$$

$$\nabla \cdot \mathbf{D} = \varrho, \tag{1.3}$$

$$\nabla \cdot \mathbf{B} = 0. \tag{1.4}$$

$\mathbf{E}$ is the electric field strength, $\mathbf{H}$ is the magnetic field strength, $\mathbf{D}$ is the electric flux density (displacement), $\mathbf{B}$ is the magnetic flux density, $\mathbf{J}$ is the electric current density, and ϱ is the electric volume charge density. The equivalent magnetic current density $\mathbf{M}$ is added to preserve the symmetry of electric and magnetic fields and currents in the curl equations. The lack of magnetic charges is manifested by zero divergence of $\mathbf{B}$ in (1.4), and the conservation of electric charge can be expressed as $\nabla \cdot \mathbf{J} = -j\omega\varrho$.

Maxwell's equations (1.1)-(1.4) have more unknowns than equations to solve the fields, and therefore we need the medium equations (constitutive relations) that are the following for linear and bi-anisotropic media:

$$\mathbf{D} = \overline{\overline{\epsilon}} \cdot \mathbf{E} + \overline{\overline{\xi}} \cdot \mathbf{H}, \tag{1.5}$$

$$\mathbf{B} = \overline{\overline{\zeta}} \cdot \mathbf{E} + \overline{\overline{\mu}} \cdot \mathbf{H}. \tag{1.6}$$

Here $\overline{\overline{\epsilon}}$ and $\overline{\overline{\mu}}$ are the material parameter dyadics (rank-2 tensors that can be expressed as matrices) and $\overline{\overline{\xi}}$ and $\overline{\overline{\zeta}}$ are the magnetoelectric dyadics [2]. The symmetry of electric and magnetic fields is seen also in the constitutive relations (1.5) and (1.6): electric polarization may rise from magnetic field and vice versa due to magnetoelectric effects. Anisotropy, or dependency on the field direction, of μ and ϵ is described through $\overline{\overline{\epsilon}}$ and $\overline{\overline{\mu}}$ and is easily seen in the microstructures of materials found from nature or in materials used in microwave engineering [3]. Therefore, anisotropic material parameters are especially handy when analysing engineered composite materials. Although magnetoelectric coupling is seldom seen in materials found from nature, it can be easily engineered and realised at microwave frequencies.

The first research problem deals with antenna miniaturisation using magnetic materials. As it is well known, the operating wavelength of a resonant antenna in free space is increased if the antenna is submerged in a host material with the relative permittivity above unity (the resonant frequency is decreased, thus the antenna imitates a physically larger antenna), and the same effect is seen if the material has the relative permeability above unity. We can ask the question: if we keep our antenna size the same and fill it with a dielectric or magnetic material, which material gives the best properties for the

antenna with reduced operational frequency? In antenna miniaturisation the bandwidth is usually degraded when the antenna is miniaturised. The bandwidth is not, however, the best figure-of-merit with lossy materials, and the radiation quality factor is used instead. Chapter 2 summarises the background and results from publications [**I**] and [**II**], and their relations to the recent advances in the field are discussed. In [**I**] it is studied what kind of antennas benefit from dielectric and magnetic material filling. A new method for determining the optimal material for a given small resonant antenna is proposed. The method is based on identifying the radiating field (equivalent current) of the antenna. In [**II**] a mobile-terminal antenna is tested with dielectric and magneto-dielectric (both dielectric and magnetic responses) materials. Guidelines for a fair comparison of filling materials in antenna miniaturisation are presented.

In the second part the antenna in question is based on a mushroom type high-impedance surface (HIS). Whereas the perfect electric conductor (PEC) has low impedance when used as a reflector, high-impedance surfaces mimic a perfect magnetic conductor (PMC). The effect is based on resonances in the surface and depends on the frequency and incident angles of the incoming wave. By using such surfaces, it has been proposed that, for example, wire antennas can be placed close and parallel to conducting surfaces—something that cannot be done normally without degrading the antenna properties. The topic has recently received a lot of interest in the literature, but still remains a difficult problem. In [**III**] the modes of an HIS are studied by using an analytical model for oblique incidence angles of the incident plane wave. Two of the resonance modes responsible for the HIS behaviour are identified and used as a basis for designing a finite antenna with two orthogonal radiation patterns. The results are summarised and discussed in Chapter 3.

A helical antenna geometry based on wires and loops is studied in the third part. By using a combination of short electric dipoles and electrically small loops acting as elementary magnetic dipoles, a Huygens' source antenna for circular polarisation (CP) from two helices is designed. Huygens' source antenna has a unidirectional radiation pattern and perfect polarisation purity: in theory it can radiate perfect CP in every direction, making it, for example, an attractive receiving antenna for space-to-Earth communications. The geometry of the antenna shows also a peculiar effect when an incoming wave is scattered from the object: The scattered field is directed away from the object when the incoming field arrives from certain directions. Chapter 4 summarises and discusses publication [**IV**] where an antenna based on this geometry is analysed

and [**V**] where the scattering from the antenna is studied.

Future research ideas are discussed at the end of each of the Chapters. Concluding remarks from the three research problems are given in Chapter 5, and a summary of the publications describing the contributions of this thesis is presented in Chapter 6.

The author of this thesis has authored or co-authored the following publications related to the three topics that are not included as parts of the thesis: [4–11].

2. Antenna miniaturisation using magnetic materials

Miniaturised radio systems have brought new wireless products for a wide audience, such as mobile terminals whose sizes are ever decreasing. Unlike waveguides and radio circuitry in radio transmitters and receivers, antennas cannot be miniaturised without sacrificing their key properties. This chapter discusses specifically resonant antennas, and miniaturisation of such antennas can be accomplished in a few ways. Take a half-wavelength wire dipole as an example. One can bend the wire so that it fits inside a smaller volume while keeping the antenna at resonance. If such miniaturisation is performed, the overall cross dimension of the antenna can become even a small fraction of the resonant wavelength, in other words, the electrical size becomes smaller. Another way to miniaturise a resonant antenna is to reduce the resonant wavelength by using a material whose relative material parameters are above unity, resulting in a smaller antenna also in terms of its electrical size. The fundamentals of small antennas are discussed first, and it will be seen that these two ways to miniaturise antennas, shaping the conductors and using non-conductive materials, have been brought together in the recent years.

2.1 Quality factor and bandwidth

The main problem in antenna miniaturisation is that whereas the size of the antenna is decreased while the radiated power is maintained, the stored energy is usually, however, increased. We can write the quality factor of a lossless antenna using the resonant circuit analogy as [12]

$$Q = \omega \frac{W}{P_{\text{rad}}}, \tag{2.1}$$

where W is the average stored energy and P_{rad} is the radiated power. The fractional bandwidth B is related to the quality factor as:

$$B = \frac{\Delta f}{f_0} = \frac{1}{Q}, \tag{2.2}$$

where f_0 is the centre frequency of the resonance and Δf is the half-power bandwidth. The fractional bandwidth is in this case inversely proportional to the stored energy, $B \propto W^{-1}$. This implies that reducing Q increases the bandwidth for resonant antennas, as long as they can be described with a similar resonant circuit model. Thus, increasing the stored energy is not desired in the miniaturisation of such antennas.

When dealing with small antennas, the radiation pattern is usually quite simple, and can be described using the elementary (Hertzian) dipole approximation. The lower limit for the quality factor of an antenna radiating like an elementary electric or magnetic dipole (sometimes referred as spherical TM_{01} and TE_{01} modes, respectively) is the so-called Chu lower bound [13–15]

$$Q_{\mathrm{Chu}} = \frac{1}{(ka)^3} + \frac{1}{ka}. \tag{2.3}$$

The dimensionless electrical sizes of antennas are often compared with the parameter ka, where $k = \omega\sqrt{\mu_0\epsilon_0}$ is the wavenumber in free space and a is the radius of the smallest sphere enclosing the antenna. In (2.3) it has been presumed that the volume inside the sphere with radius a can store energy that is needed to make the antenna self-resonant [16]. The spherical TM_{01} and TE_{01} modes or elementary dipoles radiate linear polarisation (LP) with the omnidirectional pattern, but the modes can be combined with right amplitudes and phases to radiate circular polarisation (CP). It turns out that the lower bound for both TM_{01} and TE_{01} modes radiating CP is about a half of the separate modes for small ka [13–15, 17]:

$$Q_{\mathrm{Chu}}^{\mathrm{TM}_{01}+\mathrm{TE}_{01}} = \frac{1}{2}\left(\frac{1}{(ka)^3} + \frac{2}{ka}\right). \tag{2.4}$$

The result is due to exactly twice the radiated power but a little more stored energy than in TM_{01} or TE_{01} case. The lower bounds (2.3) and (2.4) can be approached, in principle, with antennas utilising the given volume (by decreasing the stored energy) as effectively as possible. Obtainable bandwidths related to TM_{01} and TE_{01} modes are discussed in [18]. Attempts to reach the Chu lower bound with spherical wire antennas have appeared in the literature [19–24].

Wire antennas approximated only by the electric surface current $\mathbf{J}_{\mathrm{s}}$ radiating the spherical TM_{01} or TE_{01} modes from the surface of a sphere, however, cannot reach the Chu lower bounds. Such antennas obey the so-called Thal lower bounds that take into account the extra stored energy inside the sphere and are for $ka \ll 1$ the following [16, 25]:

$$Q_{\mathrm{Thal}}^{\mathrm{TM}_{01}} = 1.5 Q_{\mathrm{Chu}}, \tag{2.5}$$

$$Q_{\mathrm{Thal}}^{\mathrm{TE}_{01}} = 3.0 Q_{\mathrm{Chu}}, \tag{2.6}$$

thus restricting the obtainable minimum Q. Hansen & Collin derived an approximate formula for the TM_{01} mode [26]:

$$Q_{\mathrm{Thal}}^{\mathrm{TM}_{01}} \approx \frac{3}{2(ka)^3} + \frac{1}{\sqrt{2}ka}. \tag{2.7}$$

The difference in the coefficients in (2.5) and (2.6) is related to the difference in the stored energy. If magnetic surface current $\mathbf{M}_\mathrm{s}$ is introduced in terms of polarisation current due to magnetic material, it is theoretically possible to overcome the Thal lower bounds and reach the Chu lower bound (2.3) with a magnetic material with high permeability and low losses [27–29]. Unfortunately, such materials are not available at the present time.

Although most of the work with these so-called low-Q antennas is related to spherical or cylindrical geometries, these fundamental limitations can be applied to electrically small antennas of arbitrary shape [28]. It has been also recently noted that (2.3) can be used as a guideline even for antennas that are not strictly electrically small [30].

2.2 Materials in antenna miniaturisation

Dielectric and magnetic materials can be used in resonant antenna miniaturisation, as discussed in Chapter 1, to decrease the operating frequency of the antenna. Also, drawing from the state-of-the-art low-Q antennas reviewed in Section 2.1, there is a need for some kind of magnetically polarisable material. Whereas dielectric materials have been used in antenna miniaturisation decades ago, see e.g. [31], magnetic materials have not been equally popular. The reason behind the distinction is the frequency dispersion and loss of magnetic materials.

Regardless of material losses related to the frequency dispersion, antennas miniaturised with magnetic materials have been used in certain applications. One can find, for example, multi-loop antennas with a ferrite core inside old valve-state radio receivers. Such use was possible because in reception the efficiency was not as important as the signal-to-noise ratio in relatively low-frequency radio receivers [12]. The use of ferrites in transmitting antennas, not to mention modern antennas in portable devices, operating in the microwave region was difficult due to losses. The circumstances have, however, started to change with the modern material manufacturing technology.

The material losses have not plagued dielectric materials at radio or microwave frequencies, but all materials are inherently dispersive and lossy at

some level. The complex material parameters are the complex permittivity

$$\epsilon = \epsilon' - j\epsilon'' = \epsilon'(1 - j\tan\delta_{\mathrm{e}}), \tag{2.8}$$

and the complex permeability

$$\mu = \mu' - j\mu'' = \mu'(1 - j\tan\delta_{\mathrm{m}}), \tag{2.9}$$

where $\tan\delta_{\mathrm{e}}$ and $\tan\delta_{\mathrm{m}}$ are the dielectric and magnetic loss tangents, respectively. In (2.8) and (2.9) the notation leads to non-negative values of ϵ'' and μ'' for passive media. In a material with material parameters (2.8) and (2.9) the real parts determine the wavelength inside the material and the imaginary parts give rise to dissipative losses and wave attenuation. Additionally, we may have electric conductivity σ in a material according to Ohm's law

$$\mathbf{J} = \sigma\mathbf{E} \tag{2.10}$$

that also causes dissipative losses. The current (2.10) is included with the source current in the Ampère–Maxwell equation (1.2). The permittivity can be therefore written using σ as

$$\epsilon = \epsilon' - j\left(\epsilon'' + \frac{\sigma}{\omega}\right). \tag{2.11}$$

The loss tangents are then

$$\tan\delta_{\mathrm{e}} = \frac{\omega\epsilon'' + \sigma}{\omega\epsilon'}, \tag{2.12}$$

and

$$\tan\delta_{\mathrm{m}} = \frac{\mu''}{\mu'}. \tag{2.13}$$

When we describe the macroscopic material parameters with the permittivity ϵ and permeability μ, we average the microscopic behaviour of the individual constituents of the material. The microscopic behaviour is included in the varying material parameter values as a function of frequency, called frequency dispersion [3], and the material parameters are functions of frequency: $\epsilon = \epsilon(\omega)$, $\mu = \mu(\omega)$. In dielectrics, the relative material parameter $\epsilon_{\mathrm{r}}(\omega) = \epsilon(\omega)/\epsilon_0$ arises from the displacement of the atom's electron cloud (negative charge) around the nucleus (positive charge) under the electric field [32]. Conductivity σ, on the other hand, is related to free electrons in the material, and is not considered frequency dispersive in the microwave region. In magnetic materials, the magnetisation and the relative permeability $\mu_{\mathrm{r}}(\omega) = \mu(\omega)/\mu_0$ come from the spin magnetic moment and motion of electrons in the atoms, and are fundamentally quantum mechanical effects [32]. From here on, the microstructures of the materials in the thesis are not considered at atomic or quantum levels, but we rely on the classical description of materials through $\mu_{\mathrm{r}}(\omega)$ and $\epsilon_{\mathrm{r}}(\omega)$.

Magnetic materials in antenna applications have been studied thoroughly after it was shown that magnetic material—without dispersion—allows the miniaturisation of a patch antenna without any reduction of the bandwidth B [33]. In addition, roughly at the same time artificial magnetic materials surfaced [34,35]. Putting these together, it was wondered if artificial magnetics can be beneficial to patch-antenna miniaturisation without degrading the bandwidth. Magnetic material response in the microwave region comes in two types: we can have magnetic response due to resonance effects in artificial magnetic composites or we can have natural magnetic materials with inherent permeability, such as ferromagnetic materials. What is common between these types of magnetic materials is that the material response can be approximated using Lorentzian-type dispersion equations.

For artificial magnetic materials based on resonant inclusions, the dispersion follows the modified Lorentzian dispersion relation:

$$\mu_\mathrm{r}(\omega) = \mu_\mathrm{s} + \frac{\Lambda\omega^2}{\omega_0^2 - \omega^2 + j\omega\Gamma}, \tag{2.14}$$

where μ_s is the static permeability, Λ is the amplitude factor ($0 \leq \Lambda \leq 1$), ω_0 is the resonance frequency of the material, and Γ is the loss factor [36]. With artificial magnetic composites we have large μ' only close to the resonance frequency ω_0 of the material where the response if very dispersive. Otherwise, μ'_r approaches unity when $\omega \to 0$, i.e., $\mu_\mathrm{s} = 1$. It turns out that the dispersive and energy-storing behaviour of the material itself, which can be composed of low-loss conductors and dielectrics, is harmful for the radiation quality factor and the bandwidth of a certain patch antenna [37], and it is better to use dispersion-free dielectric materials.

However, in natural magnetic materials μ'_r can be well above unity at low frequencies ($\mu_\mathrm{s} > 1$), far away from the magnetic resonance. The reason behind the frequency dispersion in the microwave region is usually the natural ferromagnetic resonance and the domain wall motion [38]. The Lorentzian dispersion relation, that describes both of these effects, can be written in the form [39]

$$\mu_\mathrm{r}(\omega) = \mu_\mathrm{s} + \frac{(\mu_\mathrm{s} - 1)\omega^2 - j\omega(\mu_\mathrm{s} - 1)\beta\omega_\mathrm{res}}{\omega_\mathrm{res}^2 - \omega^2 + j\omega\beta\omega_\mathrm{res}}, \tag{2.15}$$

where ω_res is the ferromagnetic angular resonance frequency and β is the damping factor. Although μ_s and ω_res are related, natural magnetic materials can in theory have permeability values well above unity in the gigahertz range without excessive material losses [36]. These materials with magnetic response at microwaves are hexagonal ferrites and ferromagnetic films. Specifically, a composite material with ferromagnetic films in a dielectric host medium was

identified as a promising bulk magnetic material [36, 38, 40]. The advantages of the layered material over bulk hexagonal ferrites include easy machinability, lightness, and low relative permittivity [36]. A composite material of ferrite powder in a dielectric host medium may be considered to overcome the mentioned drawbacks, but at the cost of decreased relative permeability.

The quality factor is a relevant quantity when characterising small antennas, as discussed above, and is therefore used as a figure of merit when comparing small antennas. Quality factor is calculated for single-resonant antennas via their impedances retrieved from measurements or simulations. A traditional method is to use the voltage standing wave ratio or S parameters with the characteristic impedance of the transmission line feeding the antenna as in [41]. An alternative method to obtain an estimate of Q via the antenna impedance can be found in [42, 43]. It should be remembered that dissipative losses of an antenna decrease the quality factor, complicating the comparison of antennas with different radiation efficiencies η_r. Therefore, the radiation quality factor [12]

$$Q_\mathrm{r} = \frac{Q}{\eta_\mathrm{r}} \tag{2.16}$$

or some similar figure-of-merit that takes into account the conduction and material losses should be used with lossy antennas ($\eta_\mathrm{r} = 1$ was assumed in Section 2.1). Usually, magnetic materials need to be weakly dispersive to reach low Q values in antenna applications, but it has been suggested that strong dispersion and high losses can be used to reduce the bounds on Q [28, 44], although antennas with very low radiation efficiency find only limited applications.

Nearly dispersion-free dielectric materials are abundant, and their uses in antenna miniaturisation have been studied also in the recent years. In [45] partial filling of a quarter-wavelength microstrip antenna with a dielectric material was considered, and its effect on the radiation Q was discussed. Dielectric cap loading of a dipole antenna was used in [46]. Antennas with magneto-dielectric materials have been recently studied experimentally, at least, in [47–56]. Previous results in antenna miniaturisation that also take into account the radiation efficiency include [57–61].

The author participated in a project where the goal was to use a magneto-dielectric material in a commercial antenna application. The project can be seen to be a follow-up of [36], included in the doctoral thesis of Ikonen [39]. Before the results of the project are summarised, let us delve a little deeper in the world of antennas. As the results of [33,36,37] concerned a specific antenna geometry, more general guidelines were needed. The next question was: given a magneto-dielectric material with higher values of μ_r' than ϵ_r', what kind of

antennas can we miniaturise with it and what kind of antennas, on the other hand, benefit more from a regular low-loss dielectric material?

2.3 Choosing between magnetic and dielectric material

Previous examples of antennas that benefit from magnetic materials used a certain antenna geometry that was analysed, and it was subsequently seen that magnetic response was desirable. In [**I**] the problem was to identify resonant antennas that benefit from magnetic materials. The challenge was to describe the effect of decreasing the stored energy (or enhancing the radiation) in practical antennas of different geometries, that can be achieved by the material loading. It was seen that quite often for small antennas one field (electric or magnetic) provides the main contribution to the radiation, whereas the other field contributes mainly to the reactive stored energy. The strategy for miniaturisation of an antenna was then to fill or cover the antenna to suppress the energy-storing field, whereas the radiating field is not diminished.

To determine the material type which will be most effective for miniaturisation of a particular antenna, we proposed to model the antenna radiation using the equivalent surface currents on a conveniently chosen surface encompassing the antenna. If the antenna radiates mostly from the electric field or from the equivalent magnetic surface current [1]

$$\mathbf{M}_\mathrm{s} = -\mathbf{n} \times \mathbf{E}, \tag{2.17}$$

or from the magnetic field (equivalent electric surface current $\mathbf{J}_\mathrm{s}$)

$$\mathbf{J}_\mathrm{s} = \mathbf{n} \times \mathbf{H}, \tag{2.18}$$

the non-radiating field can be modified using magnetic or dielectric material loading, respectively, without significantly affecting the radiation process. The material loading should, of course, diminish the amplitude of the field contributing less to radiation. Two examples, though with dispersion-free materials, were used to rationalise the method.

Dipole antenna

Let us consider a dipole antenna, as shown in Fig. 2.1. This structure radiates from the electric current $\mathbf{J}$ or, by using the Huygens' principle (the equivalence principle), from the equivalent current on S created by the magnetic field: The electric field $\mathbf{E}$ is normal to the conducting cylinder and therefore also mostly normal to a virtual surface S located close to the antenna. This leads to an

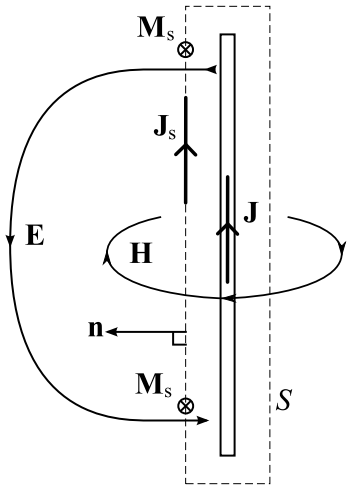

Figure 2.1. Dipole antenna embedded within a surface S. From [**I**].

insignificant equivalent magnetic current $|\mathbf{M}_\mathrm{s}| \ll |\mathbf{J}_\mathrm{s}|$ on S, and we see that the electric surface current is the main radiation mechanism.

If we want to miniaturise the antenna, $\mathbf{J}_\mathrm{s}$ caused by the magnetic field is preserved when the volume V bounded by S is filled with a dielectric material. Therefore, miniaturisation is possible without disturbing the radiating electric current. Magnetic loading also leads to miniaturisation, but simultaneously also to a decrease of the bandwidth. In practice, the bandwidth also somewhat decreases with a dielectric coating [31], but this effect is much stronger with magnetic coating.

Patch antenna

For an opposite example in terms of the radiation mechanism, assume a simple cavity model for the patch antenna with a PEC ground plane and patch, as seen in Fig. 2.2. By neglecting the fringing fields using the PMC boundary condition at the aperture surrounding the cavity, we have vertical electric field across the sidewalls of the cavity and magnetic equivalent surface current $\mathbf{M}_\mathrm{s}$ at the walls [12]. The electric surface current density $\mathbf{J}_\mathrm{s}$ in the top patch is relatively weak when the patch height is small. Also, $\mathbf{J}_\mathrm{s}$ is parallel to the ground plane, thus leading to an out-of-phase image current. Hence, the electric surface current contributes weakly to radiation.

Since the electric surface current does not produce much radiation, this structure radiates mostly from the magnetic equivalent current $\mathbf{M}_\mathrm{s}$ at the aperture. Now, magnetic filling can be used for miniaturisation without affecting the radiating electric field. As it happens, in case of a $\lambda/2$ patch antenna, the electric fields at the patch ends actually do not suffer at all from magnetic filling when compared to dielectric filling, as shown in [62] in theory and with simulation.

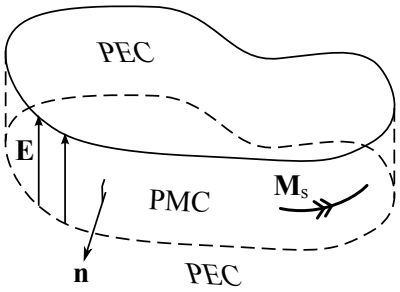

Figure 2.2. Patch antenna. From [**I**].

The current and hence the magnetic field under the patch is on the other hand reduced. Like in the previous case, the optimal material loading miniaturises the antenna (reduces the wavelength of the resonance mode).

2.4 Layered magneto-dielectric material

In relation to the guidelines presented in [**I**], an antenna miniaturisation test was carried out in [**II**]. The antenna type was chosen with today's mobile device applications in mind, and also so that it would benefit from magnetic materials. A reference miniaturisation scheme using ordinary, but high quality, dielectric material was devised for the antenna. The study used state-of-the-art magneto-dielectric material composed of thin ferromagnetic films with relatively low losses below 1 GHz.

The magneto-dielectric material was manufactured by the Institute of Theoretical and Applied Electromagnetics (ITAE) of the Russian Academy of Sciences in Moscow. The technology used produced multilayer films of Fe-N with SiO_2 interlayers on a Mylar substrate. The electromagnetic response of the material films was anisotropic with the magnetic response along the film plane. Bulk material samples were produced by stacking and gluing such films on top of each other, as seen in Fig. 2.3. Uniaxial magnetic response was ensured by laminating the films in two directions in a plane, leaving the vertical direction without magnetic response. Thus, the magneto-dielectric material has a complex response and we will describe it using the anisotropic material parameters

$$\bar{\bar{\epsilon}} = \begin{pmatrix} \epsilon_\parallel & 0 & 0 \\ 0 & \epsilon_\parallel & 0 \\ 0 & 0 & \epsilon_\perp \end{pmatrix}, \tag{2.19}$$

where $\epsilon_\parallel$ is the permittivity parallel to the films and $\epsilon_\perp$ normal to the films, and

$$\bar{\bar{\mu}} = \begin{pmatrix} \mu_\parallel & 0 & 0 \\ 0 & \mu_\parallel & 0 \\ 0 & 0 & \mu_\perp \end{pmatrix}, \tag{2.20}$$

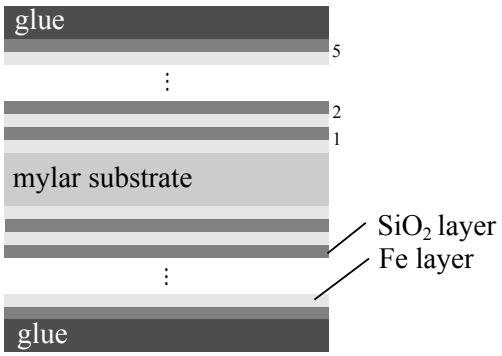

Figure 2.3. Bulk magneto-dielectric material. From [**II**].

where $\mu_\parallel$ is the permeability parallel to the films and $\mu_\perp$ normal to the films. The "uniaxial" response means that the direction normal to the films is a special direction with different material parameters than in the other directions. The parameters (2.19) and (2.20) can be written using the dyadic notation as $\overline{\overline{\epsilon}} = \epsilon_\parallel \overline{\overline{I}}_\mathrm{t} + \epsilon_\perp \mathbf{u}_\mathrm{n}\mathbf{u}_\mathrm{n}$ and $\overline{\overline{\mu}} = \mu_\parallel \overline{\overline{I}}_\mathrm{t} + \mu_\perp \mathbf{u}_\mathrm{n}\mathbf{u}_\mathrm{n}$, where $\mathbf{u}_\mathrm{n}$ is the direction normal to the films and $\overline{\overline{I}}_\mathrm{t} = \overline{\overline{I}} - \mathbf{u}_\mathrm{n}\mathbf{u}_\mathrm{n}$ is the transverse unit dyadic. The unit dyadic $\overline{\overline{I}}$ is a dyadic that relates any vector to itself as $\overline{\overline{I}} \cdot \mathbf{a} = \mathbf{a}$.

The thickness of the Fe-N and SiO_2 layers was 0.07 μm and the thickness of the Mylar substrate was 12 μm. Fe-N layers providing the magnetic response make only 3.5% of the volume of the bulk material. However, Fe-N layers are conductive, and add up to the complex permittivity (2.11). We can estimate its effect on the dielectric response using averaging methods for layered media when the layers are thin compared to the wavelength [63]. The effective permittivity parallel to the films can be calculated from

$$\epsilon_\parallel = \frac{\epsilon_1 d_1 + \epsilon_2 d_2}{d_1 + d_2}, \tag{2.21}$$

and normal to the films from

$$\epsilon_\perp = \frac{d_1 + d_2}{d_1/\epsilon_1 + d_2/\epsilon_2}, \tag{2.22}$$

where we average the parameters of the two slabs with the thicknesses d_1 and d_2 and the permittivities ϵ_1 and ϵ_2, respectively. When the material has more layers, as it is the case here, the effective parameters can be calculated in parts. It should be noted that whereas the effective permittivity can be calculated by "diluting" the conducting effect of the Fe-N films, it is not necessarily physically correct to assign some value of μ for pure Fe-N (something in the order of thousands for ferromagnetic materials) and average that with the dielectrics, as the effect of the magnetic response at microwave frequencies with this material arises from the specific thin-sheet geometry (see [36, 38]). Approximate anisotropic bulk dielectric material parameters can be calculated from (2.21) and (2.22) and then used, e.g., in full-wave simulations.

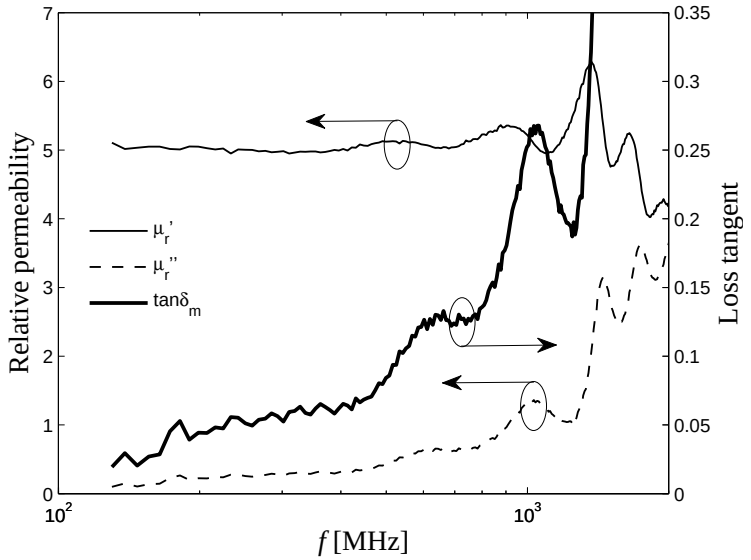

Figure 2.4. Typical values of measured relative permeability from the magneto-dielectric material samples. From [**II**].

The magneto-dielectric material was characterised by ITAE [40]. Typical values of the measured relative permeability parallel to the films are seen in Fig. 2.4. The curve is not of a purely Lorentzian type, but it can be described using a sum of Lorentzian terms [38]. The relative permeability was found to be around $\mu_{\mathrm{r}}' = 5$ with the magnetic loss tangent $\tan\delta_{\mathrm{m}} = 0.08$ at 500 MHz, whereas the relative permittivity normal to the films was $\epsilon_{\mathrm{r}} = 2.2 \ldots 2.4$ with the dielectric loss tangent $\tan\delta_{\mathrm{e}} = 0.01$, thus making it attractive for patch-type-antenna miniaturisation where electric and magnetic fields have specific spatial distributions.

2.5 Magneto-dielectric and dielectric materials in an antenna

Due to manufacturing reasons, the amount of magneto-dielectric material was not enough to fill an entire half- or quarter-wavelength patch antenna operating at around 500 MHz. Also bounded by the usual sizes of portable devices, a meandered planar inverted-F antenna (PIFA) was chosen as a test antenna for a comparison of the performance of the magneto-dielectric material against a commercial dielectric material. See Fig. 2.5 for a photograph of the antenna. The antenna is of a single and self-resonant type with the resonance frequency at $f_0 = 619$ MHz (see [**II**] for details). And importantly, the field distribution inside the patch resembles that of a quarter-wave patch antenna, thus allowing to determine the radiating mechanism (see Section 2.3). The electrical size of the antenna without the ground plane (100 mm × 40 mm) elongated in one

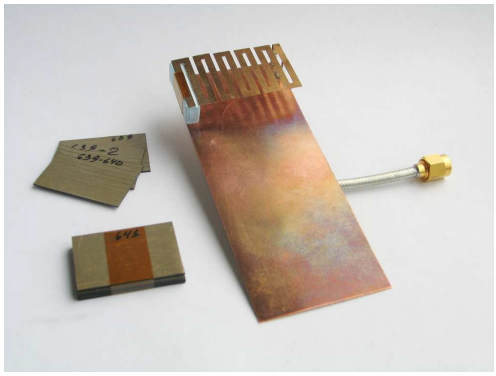

Figure 2.5. The measured antenna with magneto-dielectric material samples. From [**II**].

direction according to a usual cell-phone chassis dimensions was $ka = 0.304$. The size of the antenna can be considered to be small and comprising only the patch and the ground plane below, because the first eigenmode of the ground-plane resonances is weakly excited at frequencies below 1 GHz.

The most beneficial partial filling places for magneto-dielectric and dielectric material samples in antennas were identified according to Fig. 2.6: The strong electric field on the left in Position B is good for dielectric loading, and strong magnetic field on the right for magnetic (magneto-dielectric) loading. The magnetic field inside the cavity was simulated and found to be directed along the patch and the ground plane. Moreover, the electric field is mostly vertical, not leading to dissipation under the patch due to σ in the magneto-dielectric material.

Fair guidelines for comparing materials for antenna miniaturisation were stressed in [**II**]. The placement of the materials; the role of dissipation by using the radiation quality factor; using the same resonance frequency; and offering a good competition for the magnetic materials are all needed to reach conclusions on the practicality of the material miniaturisation.

Measurement results are presented in Fig. 2.7 for the meandered PIFA with the fabricated magneto-dielectric material and compared to the reference dielectric material filling according to the guidelines of [**II**]. The relative radiation quality factor

$$Q_{\mathrm{r}}^{\mathrm{rel}} = \frac{Q_{\mathrm{r}}^{\mathrm{diel}}}{Q_{\mathrm{r}}^{\mathrm{magn}}} \tag{2.23}$$

was used to compare the radiation quality factors with dielectric and magneto-dielectric loadings, $Q_{\mathrm{r}}^{\mathrm{diel}}$ and $Q_{\mathrm{r}}^{\mathrm{magn}}$, respectively. The quality factors with black markers were calculated from the measurements using the method described in [41] and the ones with the gray markers with [42, 43]. If the magneto-dielectric material performs better, $Q_{\mathrm{r}}^{\mathrm{rel}} > 1$, otherwise the dielectric material is more suitable. It was seen that the benefit from the magneto-dielectric mate-

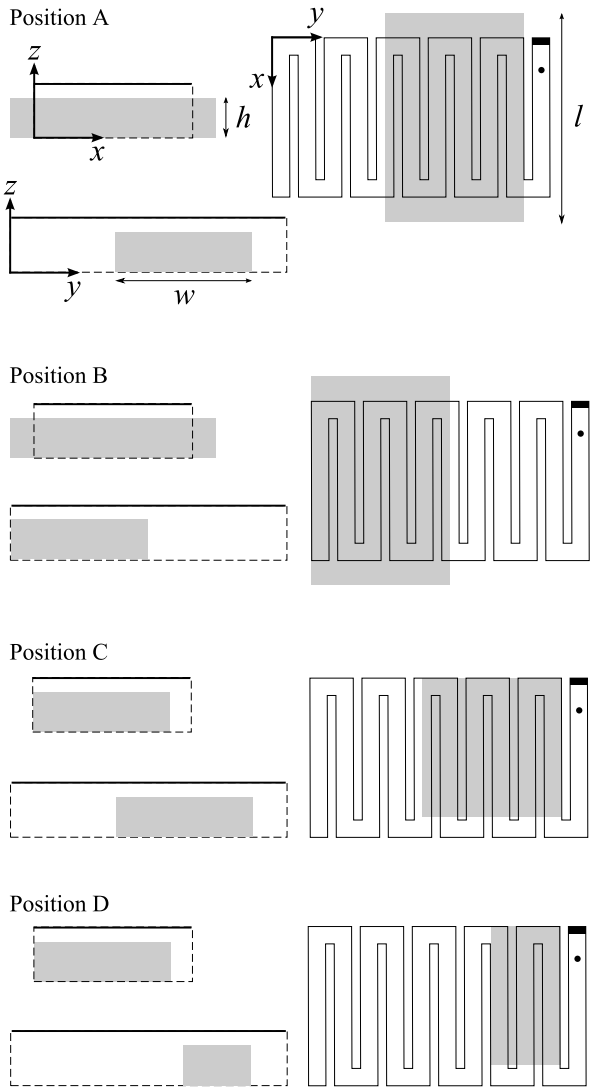

Figure 2.6. The placement of the magneto-dielectric material inside the antenna. From [**II**].

rial over the dielectric reference is strongly dependent on the positioning of the material sample. Some improvement in the radiation quality factor with the magneto-dielectric material was seen, although it was not strong. The reasons behind this can be the dielectric response of the magnetic material; the strong current in the grounding strip in the upper right corner of the patch (according to Section 2.3, the radiating wire benefits from dielectric material around it!); and the distribution of the magnetic field that is not very confined nor strong only under the patch.

2.6 Discussion and future research

Magnetic materials with high permeability and low losses are in clear demand for antenna miniaturisation. Low-Q electric and magnetic dipole antennas reviewed in Section 2.1 realised by electric surface current have different obtain-

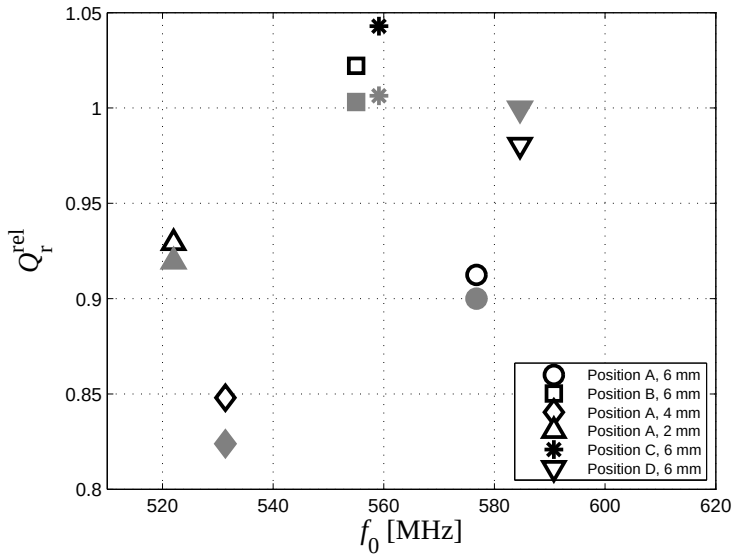

Figure 2.7. Measured Q_r^{rel} with magneto-dielectric material blocks with height h in different positions. From [**II**].

able Thal lower bounds for Q, demonstrating the discrepancy between electric and magnetic sources. Recent results have shown that by using magnetic polarisation current via magnetic materials the theoretical Chu lower bound for Q can be achieved. It can be said that magnetic materials play an important and fundamental role in the miniaturisation of single resonant antennas because we are limited by electric currents and conductors due to the restrictions from nature.

A little earlier in time, magnetic materials were found beneficial in patch antenna miniaturisation. It has been debated whether artificial and resonant magnetic materials can be at all used in antenna miniaturisation (when compared to dielectric material, for example), and the answer is no, at least in the case of half-wavelength patch antenna [36]. Current knowledge suggests that real magnetic materials with low dispersion and losses in the operating band should be used. One can imagine that dispersion plays also a role in the magnetic material used in low-Q antennas.

The emerging interest in low-Q antennas with magnetic materials, due to their novelty, has not been directly related to antenna miniaturisation with magnetic materials studied in this thesis. It is therefore relevant to question whether the guidelines presented in Section 2.3 parallel to those in Section 2.1. However, it is not easy to answer this question because the geometries and electrical sizes are somewhat different. As the guidelines of this thesis were drawn for the usual antenna geometries of wire dipole antenna (electric equivalent radiating current) and patch antenna (magnetic equivalent radiating current),

the connection to spherical or cylindrical geometries is not straightforward. When we compare the state-of-the-art low-Q electric dipole antenna of [29] to our guidelines, there seems to be still an agreement. The cap-loaded dipole of [29] would correspond to an antenna with a radiating magnetic current, and the proper material to be used in miniaturisation is a magnetic material according to this thesis. Another paper [16] presents a spherical antenna radiating the magnetic dipole mode from electrical surface current. There the conclusion is also to use magnetic materials inside the sphere that would seem to contradict the guidelines of this thesis. Thus, there are some differences if we extend the guidelines to spherical geometries and very small antenna sizes, and there is a place for future research.

The magneto-dielectric material type used in the antenna miniaturisation in [**II**] can find applications in low-Q antennas, such as those in [29] where high μ_{r}' but low ϵ_{r}' are needed, if lower losses and higher static permeability values are obtained. The research field of low-Q antennas is active and new papers are written as we speak [64, 65].

Antennas for mobile terminals generally do not use substrates or antenna carriers because of the miniaturisation effect, but out of necessity for mechanical robustness, ease of assembly, etc. Mobile terminals use often multi-resonant antennas, thus utilising the given volume better for wider bandwidth, because the additional resonances can be created with high-Q resonators coupled to the antenna. The additional resonators can be designed to be very small when compared to the radiator [66]. Further, the additional resonators can be implemented by an external reactive matching network using lumped reactive components. Also, a conducting device chassis can be coupled to a small antenna and tuned to resonance at lower cellular frequencies below 1 GHz, [67–69]. In the case of single-resonant antennas, the theory of low-Q antennas may provide new antenna types with better bandwidth, and maybe in the future antenna miniaturisation using magnetic materials will become feasible.

The use of passive materials, shaping the antenna geometry, and reactive matching networks are not the only options to miniaturise single-resonant antennas. Active tuning circuits can be used to compensate the capacitive impedance of a short wire dipole. These so-called non-Foster matching networks can have one or more active circuit elements [70–72]. Electrically small antennas other than short wire dipoles with active matching elements appear, for example, in [73, 74].

All in all, material miniaturisation of a given antenna type with either dielectric or magnetic material is a complicated task, and exact results have been

derived only for certain geometries. Experience has shown that it is good to keep the designed antennas as simple as possible, especially for commercial applications. In fact, material miniaturisation may not prove to be the best and most feasible choice in antenna miniaturisation in all circumstances [75]. On the other hand, as discussed above, extreme miniaturisation of resonant conducting antennas needs some kind of magnetic material.

3. Multimode antenna based on a high-impedance surface

Perfect electric conductor (PEC) is a useful approximation for microwave responses of conductors whose conductivities are very high, such as silver, copper, and gold. The boundary conditions for PEC set the tangential electric field to zero on the surface. This poses some limitations with respect to antennas. For example, a wire antenna located parallel and close to a conducting surface is a poor radiator. We can formulate the image principle for PEC and perfect magnetic conductor (PMC), seen in Fig. 3.1. Monopole antennas take advantage of the in-phase electric image current below PEC whereas patch antennas radiate through the in-phase magnetic equivalent current below PEC [12]. If magnetic charges and conductors were available, we could place a magnetic wire antenna close and parallel to electrical conductor without degrading the performance. In the dual case, an electric wire antenna could be placed upon a magnetic conductor surface.

However, as magnetic equivalent currents are created via electric currents, effects resembling magnetic conductors can be created using resonant structures. Sievenpiper devised such a structure in [76], called a high-impedance surface (HIS). Other names include artificial impedance surface, artificial magnetic conductor, and electromagnetic band-gap structure. Early theoretical in-

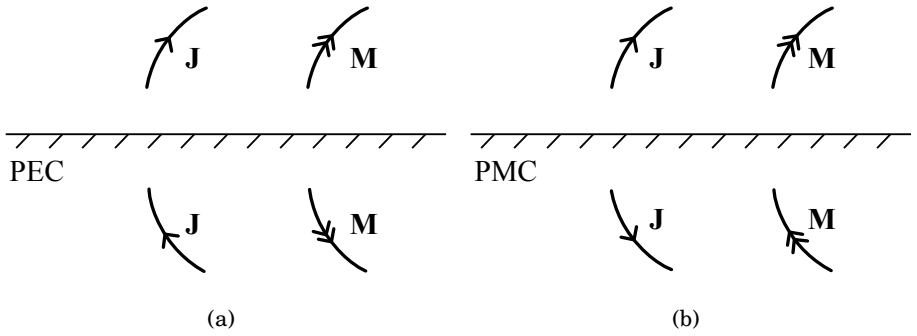

Figure 3.1. Image currents for (a) PEC and (b) PMC. Vertical components are in phase with electric (magnetic) sources inside PEC (PCM). Corresponding horizontal components are out of phase.

vestigations of radiators on an impedance surface appear in [77,78], followed by numerous papers about applications. In the following, the analysis of an infinite periodic HIS itself is based on the doctoral thesis of Luukkonen [79] where the reader is guided for more information on artificial impedance surfaces and their applications as antenna substrates.

The antenna application studied in this thesis is not a traditional one normally used with HISs, but the design philosophy is quite the opposite. Traditionally, a HIS is designed to operate at some frequency band, and then a resonant antenna also resonating at close frequencies is placed on top of it (e.g., [80]). The problem is unfortunately not an easy one to solve, because the HIS is usually designed for normal-incidence plane wave reflection, whereas a nearby antenna theoretically creates many plane-wave components, called spatial harmonics that are not generally normal to the surface. Different incidence angles upon high-impedance surfaces are thus of interest and studied in [81, 82]. The resulting radiating structure comprises both the antenna element and the HIS, and effective radiation is potentially produced close to the resonances of the antenna; the HIS excited by the spatial harmonics from the antenna; surface waves propagating on the HIS away from the antenna [83,84]; and edge diffractions at the edges of the HIS. It was proposed in [8,9] to design an antenna from the opposite point of view: If we solve the modes in the HIS suitable for producing radiation, we can use this knowledge to design and optimise the antenna structure.

Conductor-backed artificial impedance surfaces can be designed to be used in antenna applications in different ways, not necessary including a dipole antenna on top. For example, two-dimensional leaky-wave antennas appear in [85, 86], antennas with a partially reflecting surface in [87], and antennas with electric tunabilities in [88, 89]. The aforementioned antennas have usually electrically large apertures and low profiles. The antenna using a HIS can be, however, made also relatively small, as we will see below. Other realisations with the similar idea to use the surface itself as the radiator include [90, 91], although the radiation mechanism is the leaky wave.

3.1 Mushroom-type high-impedance surface

The periodic structure considered in [**III**] consists of patch-loaded posts extending from a conducting surface, and it is also called the mushroom-type HIS. The periodicity pattern can be, for example, hexagonal or square. A square HIS is seen in Fig. 3.2, and the analytical model for the HIS can be found in [82],

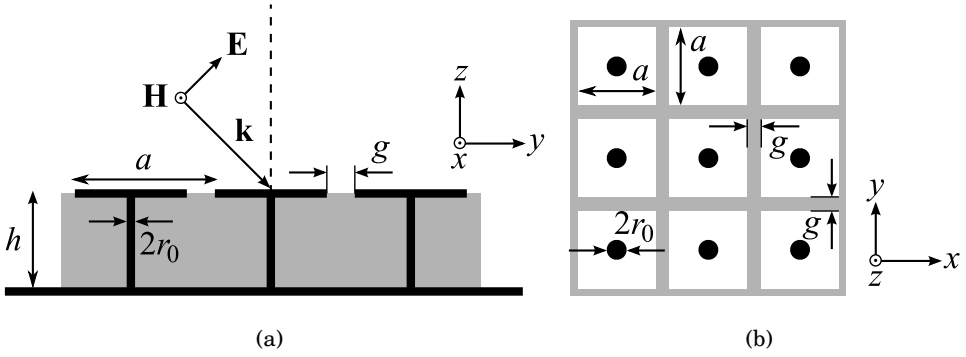

Figure 3.2. Mushroom-type high-impedance surface. (a) Side view. (b) Top view. After [82].

where the structure is analysed using a capacitive surface impedance model for the array of patches and a wire medium in a dielectric host matrix for the vias through the substrate.

When high-impedance surfaces are used as substitutes for PMC, the reflection phase of zero is a natural way to find the frequencies where the surfaces work as intended (for PEC the reflection phase is 180 degrees). If the surface is lossless, the reflection coefficient would be $\rho = -1$ for conducting surfaces and $\rho = +1$ for high-impedance surfaces. The reflection coefficient for the magnetic field for a mushroom-type HIS is found from [82]. The resonance frequencies of interest can be solved via ρ, and full-wave simulations can be used to study the wavemodes.

The dimensions for the HIS used in [**III**] can be seen in Fig. 3.2 and are the following: The period of the patch grid is $a = 20$ mm, the gap width $g = 0.5$ mm, the substrate height $h = 6.35$ mm and relative permittivity $\epsilon_\mathrm{r} = 2.33$, and the via radius $r_0 = 0.6$ mm. The reflection phase is first calculated for a normal-incidence plane wave, and it is seen in Fig. 3.3. The curve corresponding to the zero-degree incidence angle crosses zero reflection phase at 2.20 GHz. This is the traditional structural resonance used in many antenna applications. When the incidence angle deviates from the normal incidence, the TM-polarised plane wave excites the vias, or the wire medium, via its electric field, and a second resonance appears. The wire medium behaves as an artificial plasma, and the so-called plasma frequency can be calculated to be at 2.64 GHz. What we know from simulations [82] and measurements [92] and see in Fig. 3.3 is that the structural resonance moves above the plasma frequency (to 2.75…3.66 GHz) and the second resonance, dubbed plasma resonance, moves below (1.90…2.15 GHz) for oblique incidence angles.

At the structural resonance frequency of an infinite HIS for the normal incidence, the macroscopic current is uniform in the capacitive grid of patches. The current continues to flow to adjacent patches across the gap as displacement

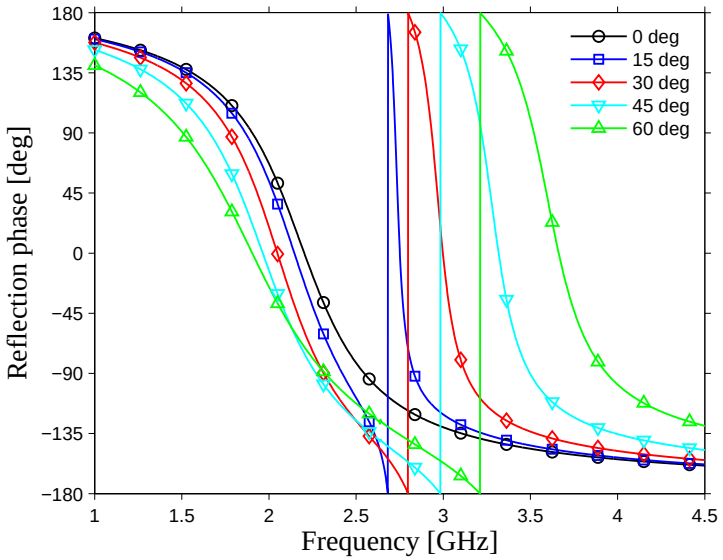

Figure 3.3. The calculated reflection phases for different incidence angles (TM plane-wave incidence). The structural resonance happens for the normal incidence angle at zero-degree reflection phase. For oblique incidence the first resonance (frequency wise) is the plasma resonance and the second one is the structural resonance. From [**III**].

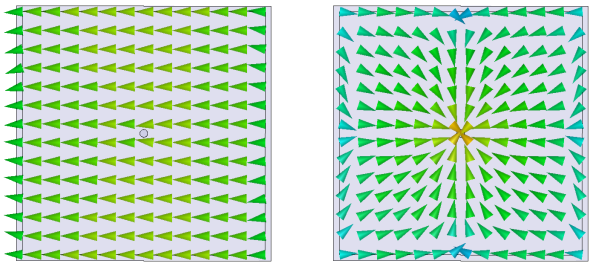

(a) (b)

Figure 3.4. Surface current modes at the patch level. (a) In the structural mode the current flows along the patches. (b) In the plasma mode the current flows along the via and is radially symmetric with respect to the centre of the patch. From [8].

current. The surface current in the structural mode is plotted in Fig. 3.4(a). At the plasma resonance frequency for oblique angles the surface current is uniform and in-phase in each via and radially symmetric in the patch, as seen in Fig. 3.4(b). In general, at the resonances seen for oblique angles in Fig. 3.3, the current mode in the structure is a superposition of the two modes of Fig. 3.4.

3.2 Finite antenna utilising two orthogonal radiating modes

Two modes in the infinite HIS were identified to be responsible for the high-impedance behaviour. The design goals for the antenna utilising the aforementioned resonance modes are good matching, sensible radiation efficiency, and distinguishable radiation patterns for both of the modes. It was noticed

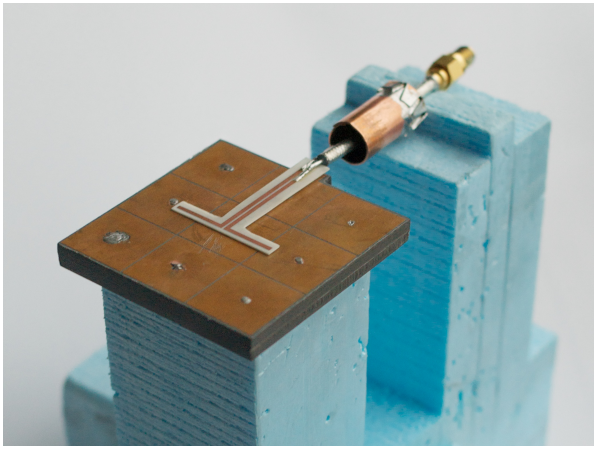

Figure 3.5. Manufactured antenna. The plasma mode is excited using the centremost via a coaxial probe (not seen in the photograph). The structural mode is excited with a dipole coupling element above the patches. From [**III**].

previously [8, 9] that a finite 3×3 unit-cell structure is enough to meet the goals. The most important finding was that we can excite the plasma and structural resonances independently at frequencies close to the ones seen in the reflection-phase calculations. The plasma resonance is excited directly from the centremost via. An electrically small port between two patches was used in [8] to excite the structural mode. A symmetrical feed for two gaps around the centre patch was designed in [9], further increasing the isolation between the ports. Thus, the antenna operating in the structural mode is basically similar to earlier realisations with dipoles over HISs, the only difference being the design philosophy and the size of the antenna.

The antenna was designed, manufactured, and measured in [**III**] and is seen in Fig. 3.5. The HIS dimensions are those used in Section 3.1 for the infinite HIS. A coaxial cable probe acting as the centremost via is used to excite the plasma mode and a dipole coupling element is used to excite the structural mode (see [**III**] for details). The dipole antenna is dubbed "coupling element" because it is designed only to couple the power to the modes of the HIS.

The measured S parameters are seen in Fig. 3.6. Now we can compare the impedance bands to the reflection phase diagram Fig. 3.3 and see that the resonance bands indeed coincide. The isolation levels are below 20 dB due to the asymmetry of the modes with respect to the feeding points. The structural resonance was previously [8, 9] a dual resonance, but now we were able to match also the third resonance with the help of positioning the dipole coupling element with the stripline waveguide. Examples of the measured directivities are presented in Fig. 3.7 (plasma mode) and Fig. 3.8 (structural mode). The plasma-mode pattern is that of a vertical electric dipole and the structural-mode pattern is similar to patch antennas without an electrically large ground

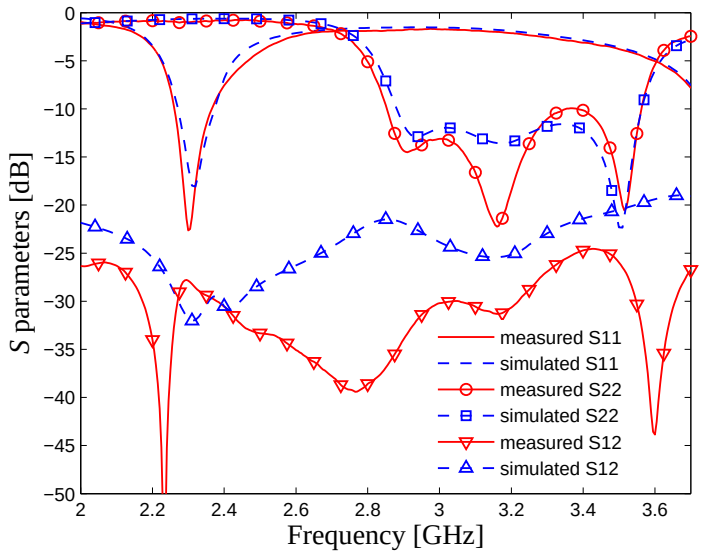

Figure 3.6. Simulated and measured S parameters. Port 1 is for the plasma mode and port 2 for the structural mode. From [**III**].

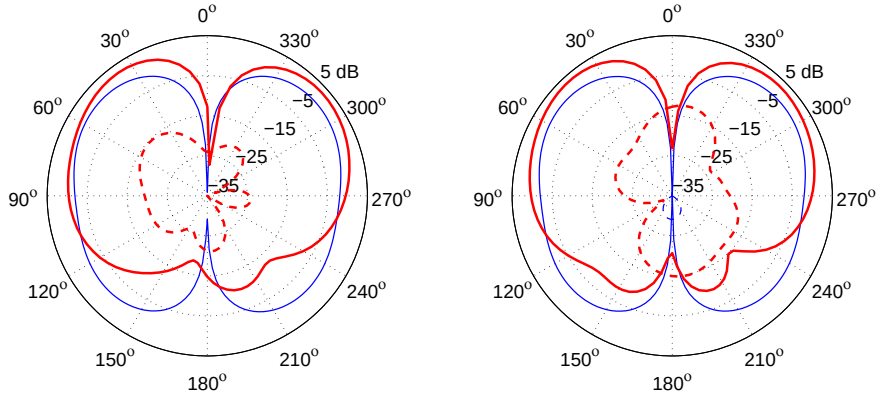

Figure 3.7. Measured (thick line) and simulated (thin line) directivity in the plasma mode at 2.30 GHz, without the dipole coupling element, at (a) xz and (b) yz planes. The cross polarisation is plotted with dashed lines. From [**III**].

plane. The patterns demonstrate, in addition to good isolation, the difference between the modes.

3.3 Discussion and future research

In addition to finding and identifying the resonance frequencies in an infinite surface, the frequencies for the plasma and the structural modes can be designed up to a degree independently from each other. As the modes are orthogonal, the antenna can be potentially used as an antenna for two radio systems.

The matching levels can be tuned for the plasma mode by changing the size

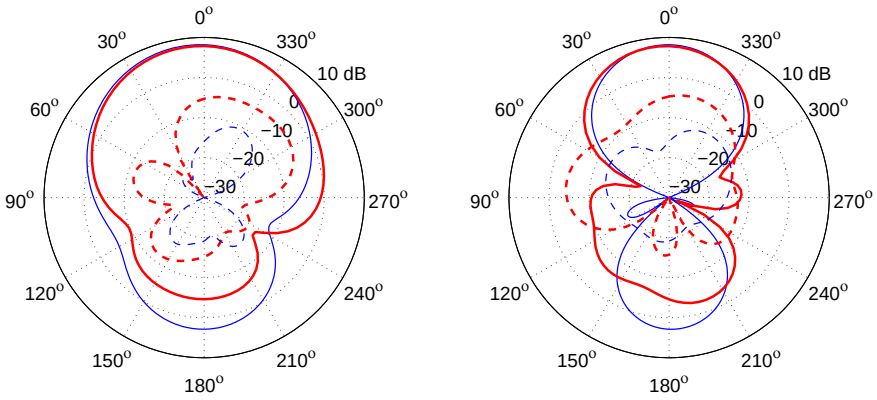

Figure 3.8. Measured (thick line) and simulated (thin line) directivity in the structural mode at 3.00 GHz, at (a) xz and (b) yz planes. The cross polarisation is plotted with dashed lines. From [**III**].

and number of the patches in the array and the height of the substrate. The measured antenna has the height of $\lambda/22$ at the plasma resonance mode, and it can be therefore seen to be a very conformal monopole-type antenna, similar to the one presented in [93]. The planar dimensions are about $\lambda/2 \times \lambda/2$.

Matching for the structural mode is related to the coupling coefficient of the coupling element to the patches. The structural mode radiates a pattern similar to a patch antenna, but with potential for a wide-band operation due to multiple resonances. The connection of the number of obtained resonances to the chosen 3×3 array of patches is a possible future research subject. The antenna was measured and designed to work in free space, but can be also made to work on a conducting surface with a small tuning in the dimensions.

In this study, the radiation mechanism was assumed to be the resonance related to the physical dimensions of the antenna. As the electrical size of the antenna was small, the study of surface waves and edge diffractions were neglected. However, leaky wave antennas with a high attenuation constant and small sizes are also a possibility, as seen in [91].

4. Huygens' antenna from helices

Dipole and loop antennas can be said to have been around in antenna technology always, from the days of Hertz's experiments. Elementary dipoles or current elements are called Hertzian dipoles, and an electrically small loop is an analogue for a magnetic elementary dipole [1]. Small helical antennas combining straight sections and loops of conducting wires, that is essentially a simplified helix, have been used in antennas for decades. In fact, the antenna geometry used often in the low-Q antennas reviewed in Section 2.1 employ wires wrapped as helices on the surface of a sphere with the radius a, effectively combining the responses from straight wires and loops. Such geometry of tightly wound spherical coils with uniform magnetic field inside were introduced by Maxwell in his famous treatise [94, pp. 304–308].

The first well-known antenna applications of the helical geometries are those of Wheeler [27, 95, 96] and Kraus [97, 98]. The polarisation of such antennas is generally elliptical, but can be also linear, depending on the winding direction. If the relation between the pitch and area of the helix and the frequency are chosen in a specific way, the polarisation of the radiated field can be purely circular, and the handedness of the helix determines the handedness of the polarisation [96].

The geometry of the so-called canonical chiral particle, simplified helix, or dipole-loop pair used in [**IV**] and [**V**] is described in Fig. 4.1, which is a simplification of an electrically small, right-handed spiral. The model was used in [99] as a simplified chiral object when the properties of chiral media were studied. Such helical objects, if electrically small, produce parallel electric and magnetic elementary dipoles $\mathbf{p}$ and $\mathbf{m}$, respectively. As discussed in Section 2.1, electrically small helical antennas are often modelled using the spherical harmonics notation, pioneered by Chu in [13]. Electric and magnetic dipoles can be described by the first two spherical harmonics components, denoted as TM_{01} and TE_{01} modes, respectively. The same fields are obtained through direct calcula-

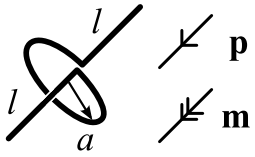

Figure 4.1. Right-handed chiral particle (helix).

tion from **p** and **m**, that is the method used in [**IV**] and [**V**]. Electric and magnetic dipoles in the origin radiate the electric field in the far zone as [100, 101]:

$$\mathbf{E} = -\omega^2 \mu_0 \frac{e^{-jkr}}{4\pi r} \mathbf{F}, \tag{4.1}$$

where the radiation vector is

$$\mathbf{F} = \mathbf{u}_r \times (\mathbf{u}_r \times \mathbf{p}) + \mathbf{u}_r \times \frac{\mathbf{m}}{\eta_0}. \tag{4.2}$$

Here $\mathbf{u}_r$ is the radial unit vector in spherical coordinates and η_0 is the free-space wave impedance. The adopted definition for electric elementary dipoles is

$$p = \frac{Il}{j\omega}, \tag{4.3}$$

where the current element or the moment of the electric dipole is Il. Magnetic dipole is defined as the moment of a small loop with a uniform current I through

$$m = \mu_0 SI, \tag{4.4}$$

where S is the area of the loop.

Paper [**IV**] models two orthogonal simplified helices as an antenna with the mentioned dipole approximation. The motivation was to realise a circularly polarised (CP) antenna with a broad beamwidth for satellite communications. The dipole pattern has two nulls, but it is possible to create the Huygens' radiation pattern with only one null. For the Huygens' pattern for linear polarisation (LP), one needs crossed electric and magnetic dipoles radiating in the same phase. For example, if **p** is x directed and **m** is y directed, the radiated waves add in phase in the $+z$ direction, but out-of-phase in the $-z$ direction, as illustrated in Fig. 4.2. The resulting pattern is thus unidirectional and the polarisation is linear in all directions. An example of Huygens' LP antenna is Green's antenna [102], which is a combination of electric and magnetic dipole antennas (dipole and a loop) using a quarter-wave phase shifter. Another name for the antenna is $P \times M$ antenna [103, 104]. An antenna with the aforementioned radiation pattern can be designed without specific phase shifters between the wire and the loop [7, 105, 106]. Another antenna type that uses crossed electric and magnetic sources is the Clavin element [107, 108].

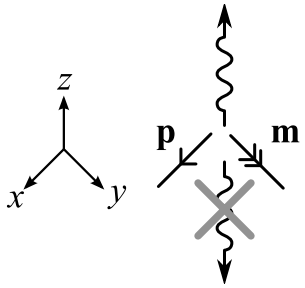

Figure 4.2. Huygens' source realised with an electric and a magnetic elementary dipole.

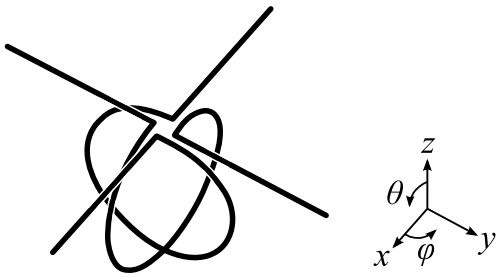

Figure 4.3. Two orthogonal helices.

For circularly polarised Huygens' antenna, two sets of electric and magnetic dipoles are needed [109]. Simply, by rotating the second set by 90 degrees in the plane of the dipoles and introducing a 90-degree phase difference, the polarisation is circular with the same pattern. Realisations of antennas resembling the Huygens' antenna for CP include [110, 111]. These crossed dipole radiators have been also studied using the spherical-harmonic notation in [112–115] for linear and circular polarisations.

4.1 Transmission and reception

In order to create a Huygens' CP antenna from two electric and two magnetic sources, one does not need four antennas. In [**IV**] it was shown that we can use two helices with a 90-degree phase shift to create this kind of an antenna. The electric dipole from the first helix and the loop from the second helix (with the phase shift) create one set of Huygens' LP source, and the rest create the second set of the source. Thus, only two helices are needed instead of four small dipoles.

We have modelled the wire dipole with a triangular current distribution and the loop with uniform current. The current at the centre of the wire is the same as the current in the loop in case of the helix. If we satisfy the condition

$$Sk = l, \tag{4.5}$$

where $S = \pi a^2$ is the area of the loop and l is the length of one dipole arm ac-

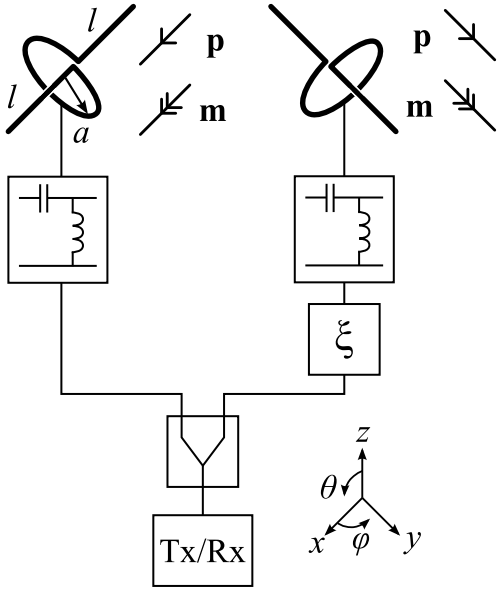

Figure 4.4. Circularly polarised antenna from two helices. Here, the helices have been draw separately. From [**V**].

cording to Fig. 4.1, the powers radiated from the wire and loop are the same. Relation (4.5) is thus essentially the same as presented in [96] for elementary dipoles. By definition, this means that the radiation resistances of the corresponding elementary dipoles are also the same.

The two helices are illustrated in Fig. 4.3, and a possible realisation of the antenna is described in Fig. 4.4, where the transmitter/receiver (Tx/Rx) is connected to the helices oriented in the x and y directions via a power divider and a phase shifter of ξ for one of the branches. Matching components can be used to match the helices to the waveguides. The transmitting/receiving pattern $\mathbf{F}_{\mathrm{rx}}$ of the antenna of Fig. 4.4 is in the spherical coordinates [**V**]

$$|\mathbf{F}_{\mathrm{rx}}|^2 = 2\left[\cos^2\theta + \cos\xi\sin 2\phi(\cos^2\theta - 1) + 2\sin\xi\cos\theta + 1\right]. \tag{4.6}$$

If the phase difference is $\xi = \pm\pi/2$, the main-beam of the antenna is in either $+z$ or $-z$ direction with a null in the opposite direction, according to

$$D = \frac{3}{4}(\cos\theta \pm 1)^2. \tag{4.7}$$

We call this the Huygens' directivity pattern. The polarisation of the antenna is theoretically circular in all directions. The antenna was simulated, manufactured and measured in [**IV**].

4.2 Scattering and absorbed power

The structure composed of two orthogonal helices has also some interesting scattering properties. It was noticed that when an incident plane wave is di-

rected normal to the plane of the particles, the backscattering magnitude is very small [10]. Scattering dipole sources induced in the particles are conveniently described by the polarisabilities as follows:

$$\mathbf{p} = \overline{\overline{\alpha}}_{\mathrm{ee}} \cdot \mathbf{E}_{\mathrm{inc}} + \overline{\overline{\alpha}}_{\mathrm{em}} \cdot \mathbf{H}_{\mathrm{inc}}, \tag{4.8}$$

$$\mathbf{m} = \overline{\overline{\alpha}}_{\mathrm{me}} \cdot \mathbf{E}_{\mathrm{inc}} + \overline{\overline{\alpha}}_{\mathrm{mm}} \cdot \mathbf{H}_{\mathrm{inc}}, \tag{4.9}$$

where $\mathbf{E}_{\mathrm{inc}}$ and $\mathbf{H}_{\mathrm{inc}}$ are the exciting fields and $\overline{\overline{\alpha}}$ are the polarisabilities written using the dyadic notation [2]. Equations (4.8) and (4.9) can be used to describe the scattering phenomenon, in principle, for all electrically small particles whose polarisabilities are known. The polarisabilities can be, in the general case, non-reciprocal, and the magnetoelectric effects for single particles are described through $\overline{\overline{\alpha}}_{\mathrm{em}}$ and $\overline{\overline{\alpha}}_{\mathrm{me}}$. A particle formed from conducting wire is naturally a reciprocal object that can have chiral- and omega-type magnetoelectric responses. The naming follows the chiral and so-called omega coupling [116] types of reciprocal magnetoelectric coupling. In chiral particles (see Fig. 4.1), electric (magnetic) field creates parallel magnetic (electric) dipoles, whereas in omega particles the fields create perpendicular dipoles.

The polarisabilities for one chiral particle are known from [117], and with $Sk = l$ they read

$$\alpha_{\mathrm{ee}} = \frac{l^2}{j\omega} \frac{1}{Z_{\mathrm{a}}}, \tag{4.10}$$

$$\alpha_{\mathrm{em}} = \pm\eta_0 \frac{l^2}{\omega} \frac{1}{Z_{\mathrm{a}}} = \pm j\eta_0 \alpha_{\mathrm{ee}}, \tag{4.11}$$

$$\alpha_{\mathrm{me}} = -\alpha_{\mathrm{em}} = \mp j\eta_0 \alpha_{\mathrm{ee}}, \tag{4.12}$$

$$\alpha_{\mathrm{mm}} = \eta_0^2 \frac{l^2}{j\omega} \frac{1}{Z_{\mathrm{a}}} = \eta_0^2 \alpha_{\mathrm{ee}}, \tag{4.13}$$

where Z_{a} is the total impedance of the particles. In (4.12) the equality is due to the reciprocity and in (4.11) the "$\pm$" sign defines the handedness of the particles: the top sign is for left handed (LH) and the bottom sign for right handed (RH) here and in the following. The electric polarisability of the loop is neglected in the analytical model for simplicity [**V**]. The missing loop polarisability for the particle geometry seen in Fig. 4.1 can be described with additional electric and omega-type polarisability components, but those are not necessarily needed for general chiral particles. For example, double and multi-filar helices do not suffer from omega coupling because of the symmetry of the geometry.

The polarisabilities of two orthogonal particles are thus

$$\overline{\overline{\alpha}}_{\mathrm{ee}} = \alpha_{\mathrm{ee}} \overline{\overline{I}}_{\mathrm{t}},$$

$$\overline{\overline{\alpha}}_{\mathrm{em}} = \alpha_{\mathrm{em}} \overline{\overline{I}}_{\mathrm{t}},$$

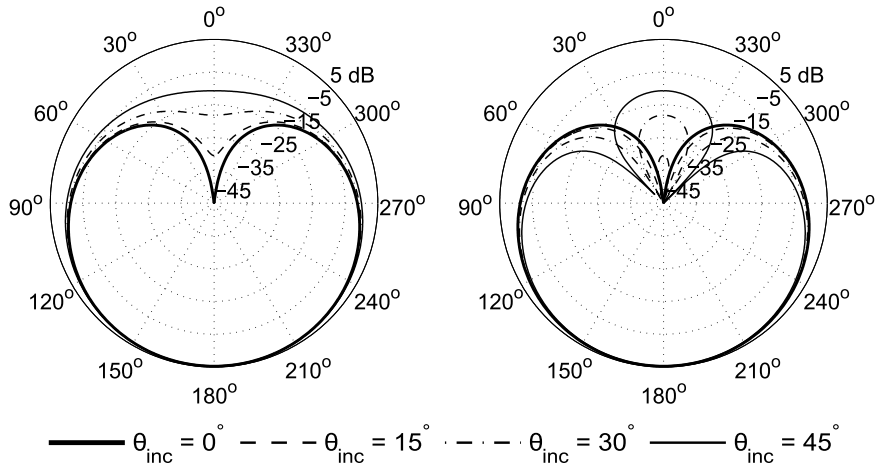

Figure 4.5. Scattering directivity from two helices. From [**V**].

$$\begin{aligned} \overline{\overline{\alpha}}_{\mathrm{me}} &= a_{\mathrm{me}} \overline{\overline{I}}_{\mathrm{t}}, \\ \overline{\overline{\alpha}}_{\mathrm{mm}} &= a_{\mathrm{mm}} \overline{\overline{I}}_{\mathrm{t}}, \end{aligned} \tag{4.14}$$

where the transverse unit dyadic is in this case $\overline{\overline{I}}_{\mathrm{t}} = \mathbf{u}_x\mathbf{u}_x + \mathbf{u}_y\mathbf{u}_y$. By using the ideal polarisabilities (4.14), we can calculate the scattered fields through $\mathbf{p}$ and $\mathbf{m}$. The directivity patterns of the scattered fields are plotted in Fig. 4.5 for a few incidence angles. We see that for the normal incidence from the $+z$ direction the scattered fields are directed towards the $-z$ direction with zero backscattering, and the same also happens with the incident direction being from $-z$ and the scattering direction being to $+z$. The simulation results for the scattering directivity are similar, as seen in [**V**]. The self-dual nature of the polarisabilities according to (4.13) with the $\pi/2$ rotational symmetry is behind the zero-backscattering phenomenon [101].

The scattered fields from the structure discussed above assumed lossless particles with some impedance Z_{a}. If we want to describe the antenna in reception, we have to connect a receiver to the particles. This is modelled as a load Z_{L} connected in the wires. The effect of Z_{L} on the scattered fields is known [12], and the resulting scattered fields were calculated in [**V**]. Also, the normalised scattering cross section was obtained as follows:

$$\sigma/\lambda^2 = \frac{1}{16\pi^2} k^4 l^4 \frac{\eta^2}{|Z_{\mathrm{a}}|^2} \left| \mathbf{F}_{\mathrm{sca}} - \frac{Z_{\mathrm{L}}}{Z_{\mathrm{L}} + Z_{\mathrm{a}}} \mathbf{F}_{\mathrm{tx}} \right|^2, \tag{4.15}$$

where $\mathbf{F}_{\mathrm{sca}}$ is the scattering pattern of the unloaded element and $\mathbf{F}_{\mathrm{tx}}$ is the scattering pattern due to Z_{L}. What was noticed is that $\mathbf{F}_{\mathrm{tx}}$ is actually also directed away from the incoming field in case of the normal incidence. This is the result of the special geometry of the antenna, and holds approximately within the dipole approximation. This means that we can set $\mathbf{F}_{\mathrm{tx}} = \mathbf{F}_{\mathrm{sca}}$, and subsequently see that (4.15) has always the same relative pattern according to $\mathbf{F}_{\mathrm{sca}}$.

This also means that power can be received to the load without backscattering. The ratio between absorbed and scattered powers P_{abs} and P_{sca}, respectively, was derived in [**V**] and is

$$\frac{P_{\mathrm{abs}}}{P_{\mathrm{sca}}} = \frac{3\pi}{8}\frac{1}{k^2 l^2}\frac{R_{\mathrm{L}}}{\eta_0}|\mathbf{F}_{\mathrm{rx}}|^2. \tag{4.16}$$

For maximum received power, the load should be the complex conjugate of the impedances of the particles. Approximating R_{a} with the known radiation resistances of electrically small loops and dipoles with triangular current distribution, and assuming resonant particles with $R_{\mathrm{L}} = R_{\mathrm{a}}$, it was shown that the ratio (4.16) depends only on the receiving pattern (4.6) as $P_{\mathrm{abs}}/P_{\mathrm{sca}} = |\mathbf{F}_{\mathrm{rx}}|^2/8$. Also, it was seen that with the Huygens' reception pattern and normal incidence $P_{\mathrm{abs}}/P_{\mathrm{sca}} = 1$, as expected according to [118]. Consequently, the antenna fulfils the limit for the maximum received power for small antennas [115].

The impedance Z_{a} was studied with full-wave simulations, and it was seen that the optimal zero-backscattering effect with unloaded particles was a little bit off resonance, at f_0, an effect that has been also noticed earlier at least in [119, 120]. The antenna impedance Z_{a} was inductive at the wanted frequency. The author, being an electrical engineer, solved the case by just tuning the positive reactance away with an additional capacitance. As the impedances of the particles are now real R_{a}, the conjugate loading was simulated with $Z_{\mathrm{L}} = R_{\mathrm{L}} = R_{\mathrm{a}}$. The simulation results with LP incidence compared to (4.15) are presented in Fig. 4.6. The lossless object has the Huygens' $\cos\theta - 1$ pattern with a null in $\theta = 0^\circ$ (incidence) direction and relatively low scattering cross section. As the object is tuned to resonance, the level naturally rises, but the shape is the same. Finally, with conjugate loading the antenna receives all the available power with low levels of backscattering. Corresponding simulation results for a dipole with the length $2l$ are shown for reference.

Fig. 4.7 shows backscattering levels for the normal incidence as a function of frequency. The result of tuning the impedance is seen: The resonance from $0.946 f_0$ is shifted to f_0 with capacitive loading, thus allowing the antenna to receive power with conjugate loading and to scatter similar magnitudes over frequency than an electrically small, non-resonant, dipole.

4.3 Zero-backscattering antenna

Reducing the scattering of antennas might be useful, for example, in sensor applications where the object under test is in close proximity [121, 122]. Unfortunately, an invisible and passive antenna is not possible due to the optical

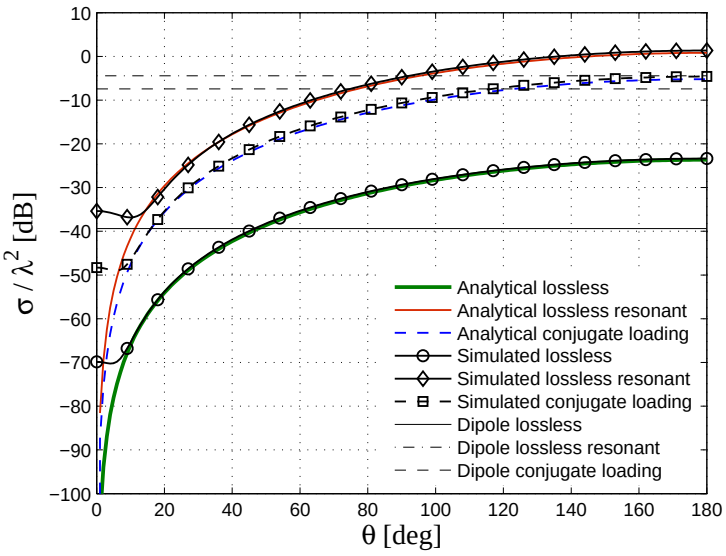

Figure 4.6. Analytical and simulated σ/λ^2 for the lossless and conjugate-loaded object with reference-dipole limits. From [**V**].

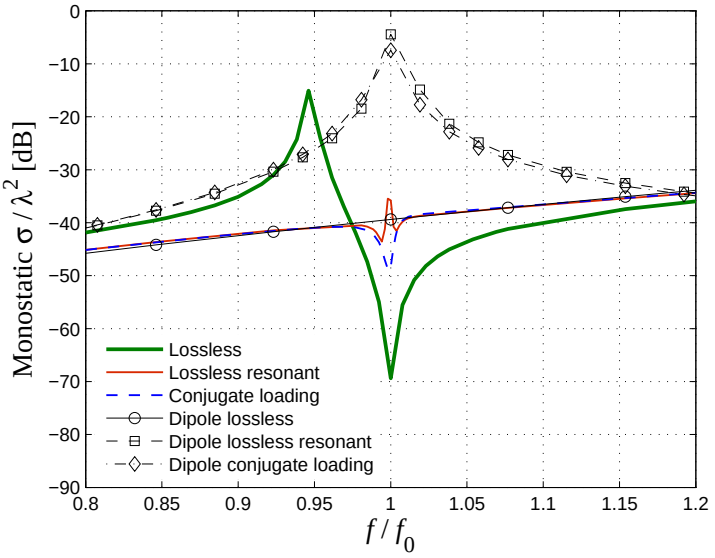

Figure 4.7. Simulated monostatic scattering cross section for normal incidence for the lossless, lossless at resonance, and conjugate-loaded element with the reference dipoles. From [**V**].

theorem [123]: If a passive object has some non-zero total scattering cross section, the forward-scattering amplitude is non-zero. This means that if an object receives some power, it must forward scatter, and perfect "cloaking" of a passive receiving antenna is not possible.

Scattered power can be decreased considerably, for example, with so-called scattering cancellation techniques [121, 122, 124, 125]. For electrically small dipole antennas the scattering is reduced at the price of the received power [125], but with more complex structures more power can be absorbed if the scattered power is directed only in the forward direction [118, 121, 122]. If all the

available power is required for sensing purposes, the best we can do with antennas utilising electric and magnetic dipoles is to allow forward scattering, but reduce backscattering. Generally, for zero backscattering of travelling waves in free space, we need a self-dual object and $\pi/2$ rotational symmetry [101] which was the case above with two orthogonal helices.

Assuming a small object realisable within the dipole approximation, the conditions for self-dual polarisabilities can be derived similarly as those for general media in [101], and it turns out that the following conditions should hold [126]:

$$\overline{\overline{\alpha}}_{\mathrm{mm}} = \eta_0^2 \overline{\overline{\alpha}}_{\mathrm{ee}}, \tag{4.17}$$

$$\overline{\overline{\alpha}}_{\mathrm{em}} = -\overline{\overline{\alpha}}_{\mathrm{me}}. \tag{4.18}$$

The first relation (4.17) dictates that the electric and magnetic responses should be similar, and an example of such object is a magneto-dielectric sphere with $\mu_{\mathrm{r}} = \epsilon_{\mathrm{r}}$. Such sphere is a zero-backscattering object for any incidence direction and polarisation. The second relation (4.18) relates the cross-polarisabilities (that can be also zero) to each other.

Let us now try to imitate an isotropic self-dual zero-backscattering object with an object composed of chiral particles or helices discussed in Section 4.2. Relation (4.17) was satisfied for two orthogonal chiral particles for the normal incidence assuming $Sk = l$. If we add a third identical particle in the orthogonal z direction, we form a self-dual object with the polarisabilities as follows:

$$\begin{aligned}
\overline{\overline{\alpha}}_{\mathrm{ee}} &= a_{\mathrm{ee}} \overline{\overline{I}}, \\
\overline{\overline{\alpha}}_{\mathrm{em}} &= a_{\mathrm{em}} \overline{\overline{I}}, \\
\overline{\overline{\alpha}}_{\mathrm{me}} &= a_{\mathrm{me}} \overline{\overline{I}}, \\
\overline{\overline{\alpha}}_{\mathrm{mm}} &= a_{\mathrm{mm}} \overline{\overline{I}},
\end{aligned} \tag{4.19}$$

where the unit dyadic is $\overline{\overline{I}} = \mathbf{u}_x\mathbf{u}_x + \mathbf{u}_y\mathbf{u}_y + \mathbf{u}_z\mathbf{u}_z$. As the dyadics (4.19) have only diagonal terms, the relation (4.18) is also satisfied for reciprocal helices. An object with these polarisabilities is an isotropic self-dual object, and it was shown in [126] that zero backscattering also holds for any incidence direction and polarisation. The polarisation of the scattered field is again fixed through (4.11) and (4.12) and it is circular, with the handedness according to the handedness of the particles. The isotropic object is an analogue of a chiral sphere with a certain value of the chirality parameter [126].

Following [**V**], an antenna system consisting of three orthogonal particles with three receivers could, in principle, realise the unidirectional Huygens' reception pattern and always scatter the power away from the incidence direction.

4.4 Discussion and future research

The chiral particles (helices) according to Fig. 4.1 were modelled as electrically small dipoles. In addition to the balance condition (4.5), it was assumed in [**V**] that the particles are at resonance by assigning the total length of the wire to be equal to half the wavelength. Following these conditions, one can determine the dimensions of the particles which are as follows:

$$kl = \frac{\pi}{4}\left(\sqrt{3}-1\right)^2, \tag{4.20}$$

$$ka = \frac{\sqrt{3}-1}{2}. \tag{4.21}$$

Relation (4.21) also appears in [120]. These results means that the structure has always the same shape and scales with the wavelength, so that the electrical length of the dipole arm $kl \approx 0.42$ and the electrical radius of the loop $ka \approx 0.27$. The particles thus belong to the category of electrically small antennas that can be fitted inside a radiansphere with the radius $\lambda/2\pi$ (within a sphere with the electrical size $ka \leq 1$) [95]. As the zero backscattering property is based on equal electric and magnetic dipole-moment magnitudes, it is a single-frequency phenomenon. The bandwidth for a level of acceptable backscattering is determined by the Q of the antenna.

In the simulations it was noticed, however, that the resonance condition was never achieved with the desired zero-backscattering effect, and capacitive loading was used. Also, the polarisation of the simulated scattered field was not circular with LP incidence, but rather elliptical (for CP incidence the scattered field was also CP due to the symmetry of the excitation). Similar behaviour has been observed, at least, in [119, 120] for single helices of the same geometry. A likely reason behind this phenomenon is related to fundamental differences between electric and magnetic excitation. As we have seen in Section 2.1, the electric and magnetic dipoles occupying the same volume affect each other. In fact, an electrically small spherical helix composed of a conducting wire (with an air core) in resonance cannot be made to radiate perfect CP, and the electric dipole radiates twice the power as the magnetic dipole [27], unless the radiated power is balanced by loading. This effect is also present in [20] where a 3-dB difference was seen between the radiated components of the elliptically polarised spherical antenna.

Although the difference in the radiated power was calculated for spherical antennas, it is also the probable reason why the scattered polarisation from LP incidence in our helical object is not circular but has the inverted axial ratio of about 0.7 [**V**], which corresponds to the 3-dB difference in [20]. When

the capacitances were added to the particles, it corresponded to the material loading of the antenna described in [25, 27], thus allowing circularly polarised radiation (but also affecting the quality factor of the antenna). The lower bound for the quality factor for the antenna composed of two orthogonal ideal helices radiating CP with the Huygens' pattern is the same as for one helix presented in (2.4), as can be derived using the method introduced by McLean in [15]. The realised Q of the antenna in [**V**] is not close to the limits in [25] because of the shape of the antenna and the additional loading. Other geometries than the simplified helix might be considered for the helical antenna in order to reach a lower Q.

5. Conclusion

This thesis addresses antennas that are related to magnetic materials, responses, and equivalent currents. In the first part, it was seen that magnetic materials play a fundamental role in miniaturisation of conducting resonant antennas. However, magnetic materials with high permeability and low losses for the miniaturisation of so-called low-Q antennas are not available at the present time. A seemingly unrelated research field uses also magnetic materials for patch antenna miniaturisation. A method for identifying a dielectric or a magnetic material for antenna miniaturisation was presented. The method was based on the model of radiating currents or fields and it was formulated for commonly used antenna types and sizes and realistic magnetic materials, thus making the comparison to low-Q antennas difficult.

A rigorous comparison of a planar inverted-F antenna with magneto-dielectric and dielectric fillings was conducted by measurements. It was seen that partial filling of the antenna cavity is enough to see differences in the radiation Q used as the figure-of-merit. The results suggest that a magnetic material with static relative permeability above unity can be used to miniaturise an antenna with better bandwidth potential when compared to a dielectric material filling. On the other hand, inappropriate positioning of the magneto-dielectric material sample does not lead to better radiation Q when compared to dielectric material fillings. In practice, an analysis of the antenna in question is needed, if a realistic magneto-dielectric material is used in antenna miniaturisation.

In the second part a HIS-based antenna was designed and manufactured. The resonance modes of the infinite-sized surface leading to the HIS-behaviour were used to design a finite, relatively small antenna. Specifically, the reflection phase diagram of an infinite surface was used to predict the resonance bands of a finite antenna. The resulting multi-mode antenna imitates a low-profile monopole antenna or a patch antenna with the ability to work close to conducting surfaces.

The third part introduced small helical antennas that were used to design a unidirectional Huygens' antenna for circular polarisation. Also, the specific antenna geometry acts as a Huygens' source for the scattered field, when the incidence direction is normal to the plane set by the axes of the helices. This property was used to design an antenna with zero backscattering and the ability to receive all the available power. An isotropic antenna of three orthogonal helices was introduced in theory, effectively with the same properties as the experimentally realised antenna. The antenna belongs to the class of electrically small low-Q antennas, as it can be modelled with dipoles, thus obeying the known fundamental limits for small antennas.

The research topics studied in this thesis are relatively active, and new research results are published yearly. For example, the values of magnetic material parameters obtained with modern-day technology are not yet close to the theoretically achievable ones. Also, the bandwidths of the helical antennas in this thesis can be perhaps increased by better antenna geometries. The applications do not need to be strictly in small antennas, as the helical geometries in Chapter 4 are currently being used in array configuration in polarisation transformers [127].

6. Summary of articles

Publication I: "Choosing dielectric or magnetic material to optimize the bandwidth of miniaturized resonant antennas"

The paper studies the optimal choice of loading material for antenna miniaturisation. A new approach to identify the optimal loading material (dielectric or magnetic) for maximization of bandwidth of resonant antennas is introduced. Instead of equivalent resonant circuits or transmission-line resonators, an analysis of radiation mechanism was is to identify the fields contributing mostly to the stored energy and determine the beneficial material type. The formulated rule is qualitatively illustrated using a dipole and a patch antenna, as well as a planar inverted-L antenna where the conventional analysis of circuit or a transmission-line resonator leads to incorrect conclusions. Guidelines are presented for miniaturising different antenna types.

Publication II: "Experimental studies of antenna miniaturization using magneto-dielectric and dielectric materials"

Dielectric or magneto-dielectric materials can be used to miniaturise antennas, but there are many important parameters that must be considered when selecting which material to use. The authors discuss these figures of merit and a rigorous method to compare antennas with different material fillings. A meandered planar inverted-F antenna (PIFA) loaded with magneto-dielectric and dielectric materials is presented as an example antenna for testing. The magneto-dielectric material used is composed of Mylar substrate and Fe-SiO_2 sheets. Measurement results for the permeability of the material are presented. The radiation mechanism of the meandered PIFA is studied, and the proper position for dielectric and magneto-dielectric filling is discussed and identified.

Miniaturisation by commercial dielectric and the presented magneto-dielectric fillings is measured and compared at the same resonance frequency using the radiation quality factor as the figure of merit. It is seen, that the antenna can benefit from the magneto-dielectric filling material in terms of the radiation quality factor only if the placement of the antenna filling is carefully selected.

Publication III: "High-impedance-surface-based antenna with two orthogonal radiating modes"

This paper summarises the results of [8,9], and validates the proposed antenna with measurements. The properties of a mushroom-type HIS using reflection-phase calculations for oblique incidence are studied and two orthogonal resonant modes are found. An antenna based on a finite-sized HIS is designed to utilise both of these modes. Measurement results are presented for the antenna, and we report two separate modes with asymmetric radiation patterns. The first mode provides a dipole-like radiation pattern and the second one a broadside pattern. Furthermore, the second mode can be coupled to the antenna with a proper coupling element in order to obtain a wide bandwidth. Both of the modes can be matched to 50-Ohm coaxial cables, and good isolation levels between the ports are seen due to the orthogonality of the modes in the HIS.

Publication IV: "Design and realisation of an electrically small Huygens source for circular polarisation"

The authors study the possibilities of realising circularly polarised Huygens' source antennas combining electric and magnetic dipoles. The required combinations of dipoles are first studied analytically. Radiating elements comprising both electric and magnetic dipoles in a single element, namely, chiral particles, are then chosen as a way to realise the required dipole radiators. The use of elements that have equally strong electric and magnetic dipoles in a single element greatly simplifies the realisation and feeding of these antennas. The designed antennas are studied numerically and finally the radiation properties of the antennas are verified with measurements. The numerical and experimental results confirm that the antennas have radiation characteristics similar to a Huygens' source.

Publication V: "Circularly polarized receiving antenna from two chiral particles with low backscattering levels"

An antenna element composed of two orthogonal helices is proposed as a low-scattering sensor. The vector effective length is derived for the element using the small dipole approximation for the chiral particles. The element can transmit and receive circular polarisation in all directions with the Huygens' pattern. We observe that the element does not backscatter, regardless of the polarisation, when the incidence direction is normal to the plane of the helices. Scattered fields, scattered axial ratio, and the scattering cross section are presented. We show that the zero-backscattering property holds also for the antenna element when it is capable to receive all the available power with conjugate loading. The approximate analytical model is validated with full-wave simulations.

Bibliography

[1] R. F. Harrington, *Time-Harmonic Electromagnetic Fields*, ser. IEEE Press Classic Reissue. New York, NY: Wiley, 2001.

[2] A. Serdyukov, I. Semchenko, S. Tretyakov, and A. Sihvola, *Electromagnetics of Bi-anisotropic Materias, Theory and Applications*. Amsterdam, The Netherlands: Gordon and Breach, 2001.

[3] A. Sihvola, *Electromagnetic Mixing Formulas and Applications*. London, UK: IET, 1999.

[4] A. O. Karilainen, P. M. T. Ikonen, C. R. Simovski, and S. A. Tretyakov, "Benefits of material loading of electrically small resonant antennas," in *Prog. Electromagn. Res. Symp. (PIERS)*, Moscow, Russia, 18-21 Aug. 2009, p. 635.

[5] A. O. Karilainen, P. Ikonen, C. R. Simovski, S. A. Tretyakov, A. N. Lagarkov, S. A. Maklakov, K. N. Rozanov, and S. N. Starostenko, "Experimental study of a planar inverted-F antenna with a magnetic substrate," in *Prog. Electromagn. Res. Symp. (PIERS)*, Moscow, Russia, 18-21 Aug. 2009, p. 913.

[6] P. Alitalo, A. Karilainen, T. Niemi, C. R. Simovski, S. A. Tretyakov, and P. de Maagt, "Chiral antennas radiating circularly polarized waves," in *Proc. 4th European Conf. Antennas Propag. (EuCAP)*, Barcelona, Spain, 12-16 Apr. 2010.

[7] P. Alitalo, A. O. Karilainen, T. Niemi, C. R. Simovski, and S. A. Tretyakov, "A linearly polarized Huygens source formed by two omega particles," in *Proc. 5th European Conf. Antennas Propag. (EuCAP)*, Rome, Italy, 11-15 Apr. 2011, pp. 2445–2448.

[8] O. Luukkonen, A. O. Karilainen, J. Vehmas, C. Simovski, and S. A. Tretyakov, "A high-impedance surface based antenna – lose the antenna," in *Proc. 4th European Conf. Antennas Propag. (EuCAP)*, Barcelona, Spain, 12-16 Apr. 2010.

[9] O. Luukkonen, A. O. Karilainen, J. Vehmas, and S. A. Tretyakov, "A tri-band low-profile antenna based on a high-impedance surface," in *Proc. IEEE Antennas Propag. Soc. Int. Symp.*, Toronto, ON, 11-17 Jul. 2010.

[10] A. O. Karilainen, P. Alitalo, and S. A. Tretyakov, "Chiral antenna element as a low backscattering sensor," in *Proc. 5th European Conf. Antennas Propag. (EuCAP)*, Rome, Italy, Apr. 11-15 2011, pp. 1983–1986.

[11] A. O. Karilainen and S. A. Tretyakov, "Zero-backscattering self-dual object from two chiral particles," in *Proc. Metamaterials 2011*, Barcelona, Spain, 10-13 Oct. 2011, pp. 405–407.

[12] C. A. Balanis, *Antenna Theory: Analysis and Design*, 3rd ed. Hoboken, NJ: Wiley, 2005.

[13] L. J. Chu, "Physical limitations of omni-directional antennas," *J. Appl. Phys*, vol. 19, no. 12, pp. 1163–1175, Dec. 1948.

[14] R. Collin and S. Rothschild, "Evaluation of antenna Q," *IEEE Trans. Antennas Propag.*, vol. 12, no. 1, pp. 23–27, Jan 1964.

[15] J. S. McLean, "A re-examination of the fundamental limits on the radiation Q of electrically small antennas," *IEEE Trans. Antennas Propag.*, vol. 44, no. 5, pp. 672–676, May 1996.

[16] O. S. Kim, O. Breinbjerg, and A. D. Yaghjian, "Electrically small magnetic dipole antennas with quality factors approaching the Chu lower bound," *IEEE Trans. Antennas Propag.*, vol. 58, no. 6, pp. 1898–1906, Jun. 2010.

[17] R. Fante, "Quality factor of general ideal antennas," *IEEE Trans. Antennas Propag.*, vol. 17, no. 2, pp. 151–155, Mar. 1969.

[18] A. Hujanen, J. Holmberg, and J. C.-E. Sten, "Bandwidth limitations of impedance matched ideal dipoles," *IEEE Trans. Antennas Propag.*, vol. 53, no. 10, pp. 3236–3239, Nov. 2005, (Erratum: IEEE Trans. Antennas Propag., vol. 54, no. 9, p. 2694, Sep. 2006.).

[19] S. R. Best, "The radiation properties of electrically small folded spherical helix antennas," *IEEE Trans. Antennas Propag.*, vol. 52, no. 4, pp. 953–960, Apr. 2004.

[20] ——, "Low Q electrically small linear and elliptical polarized spherical dipole antennas," *IEEE Trans. Antennas Propag.*, vol. 53, no. 3, pp. 1047–1053, Mar. 2005.

[21] A. Erentok and R. W. Ziolkowski, "Metamaterial-inspired efficient electrically small antennas," *IEEE Trans. Antennas Propag.*, vol. 56, no. 3, pp. 691–707, Mar. 2008.

[22] S. R. Best, "A low Q electrically small magnetic (TE mode) dipole," *IEEE Antennas Wireless Propag. Lett.*, vol. 8, pp. 572–575, Jul. 2009.

[23] O. S. Kim, "Low-Q electrically small spherical magnetic dipole antennas," *IEEE Trans. Antennas Propag.*, vol. 58, no. 7, pp. 2210–2217, Jul. 2010.

[24] A. Erentok and O. Sigmund, "Topology optimization of sub-wavelength antennas," *IEEE Trans. Antennas Propag.*, vol. 59, no. 1, pp. 58–69, Jan. 2011.

[25] H. L. Thal, "New radiation Q limits for spherical wire antennas," *IEEE Trans. Antennas Propag.*, vol. 54, no. 10, pp. 2757–2763, Oct. 2006.

[26] R. C. Hansen and R. E. Collin, "A new Chu formula for Q," *IEEE Antennas Propag. Mag.*, vol. 51, no. 5, pp. 38–41, Oct. 2009.

[27] H. A. Wheeler, "The spherical coil as an inductor, shield, or antenna," *Proc. IRE*, vol. 46, no. 9, pp. 1595–1602, Sep. 1958.

[28] A. D. Yaghjian and H. R. Stuart, "Lower bounds on the Q of electrically small dipole antennas," *IEEE Trans. Antennas Propag.*, vol. 58, no. 10, pp. 3114–3121, Oct. 2010.

[29] H. R. Stuart and A. D. Yaghjian, "Approaching the lower bounds on Q for electrically small electric-dipole antennas using high permeability shells," *IEEE Trans. Antennas Propag.*, vol. 58, no. 12, pp. 3865–3872, Dec. 2010.

[30] D. Sievenpiper, D. Dawson, M. Jacob, T. Kanar, S. Kim, J. Long, and R. Quarfoth, "Experimental validation of performance limits and design guidelines for small antennas," *IEEE Trans. Antennas Propag.*, vol. 60, no. 1, pp. 8–19, Jan. 2012.

[31] D. Lamensdorf, "An experimental investigation of dielectric-coated antennas," *IEEE Trans. Antennas Propag.*, vol. 15, no. 6, pp. 767–771, Nov 1967.

[32] R. P. Feynman, R. B. Leighton, and M. Sands, *The Feynman Lectures on Physics, Volume II: Mainly Electromagnetism and Matter*. New York: Basic Books, 2010.

[33] R. C. Hansen and M. Burke, "Antennas with magneto-dielectrics," *Microwave Opt. Technol. Lett.*, vol. 26, no. 2, pp. 75–78, Jul. 2000.

[34] M. V. Kostin and V. V. Shevchenko, "Artificial magnetics based on double circular elements," in *Proc. Bianisotropics'94*, Périgueux, France, 18-20 May 1994, pp. 49–56.

[35] J. Pendry, A. Holden, D. Robbins, and W. Stewart, "Magnetism from conductors and enhanced nonlinear phenomena," *IEEE Trans. Microw. Theory Tech.*, vol. 47, no. 11, pp. 2075–2084, Nov. 1999.

[36] P. M. T. Ikonen, K. N. Rozanov, A. V. Osipov, P. Alitalo, and S. A. Tretyakov, "Magnetodielectric substrates in antenna miniaturization: Potential and limitations," *IEEE Trans. Antennas Propag.*, vol. 54, no. 11, pp. 3391–3399, Nov. 2006.

[37] P. M. T. Ikonen, S. I. Maslovski, C. R. Simovski, and S. A. Tretyakov, "On artificial magnetodielectric loading for improving the impedance bandwidth properties of microstrip antennas," *IEEE Trans. Antennas Propag.*, vol. 54, no. 6, pp. 1654–1662, Jun. 2006.

[38] A. N. Lagarkov and K. N. Rozanov, "High-frequency behavior of magnetic composites," *J. Magnetism Magn. Materials*, vol. 321, pp. 2082–2092, 2009.

[39] P. Ikonen, "Artificial electromagnetic composite structures in selected microwave applications," Doctoral thesis, Helsinki University of Technology, 2007. [Online]. Available: http://lib.tkk.fi/Diss/2007/isbn9789512286775/

[40] A. N. Lagarkov, S. A. Maklakov, A. V. Osipov, D. A. Petrov, K. N. Rozanov, I. A. Ryzhikov, M. V. Sedova, S. N. Starostenko, and I. T. Yakubov, "Properties of layered structures based on thin ferromagnetic films," *J. Communications Techn. Electronics*, vol. 54, no. 5, pp. 596–603, 2009.

[41] H. Pues and A. Van de Capelle, "An impedance-matching technique for increasing the bandwidth of microstrip antennas," *IEEE Trans. Antennas Propag.*, vol. 37, no. 11, pp. 1345–1354, Nov. 1989.

[42] A. Yaghjian and S. Best, "Impedance, bandwidth, and Q of antennas," *IEEE Trans. Antennas Propag.*, vol. 53, no. 4, pp. 1298–1324, Apr. 2005, (Erratum: IEEE Trans. Antennas Propag., vol. 55, p. 3748, 2007.).

[43] A. Yaghjian, "Improved formulas for the Q of antennas with highly lossy dispersive materials," *IEEE Antennas Wireless Propag. Lett.*, vol. 5, no. 1, pp. 365–369, 2006.

[44] A. D. Yaghjian, “Internal energy, Q-energy, poynting’s theorem, and the stress dyadic in dispersive material,” *IEEE Trans. Antennas Propag.*, vol. 55, no. 6, pp. 1495–1505, Jun. 2007, (Erratum: IEEE Trans. Antennas Propag., vol. 55, p. 3748, 2007.).

[45] O. Luukkonen, P. Ikonen, and S. Tretyakov, “Microstrip antenna miniaturization using partial dielectric material filling,” *Microwave Opt. Technol. Lett.*, vol. 49, no. 1, pp. 155–159, Jan. 2007.

[46] M. Hirvonen, “Dielectric cap loading technique for improving the antenna element performance,” *IEEE Antennas Wireless Propag. Lett.*, vol. 10, pp. 431–434, 2011.

[47] T. Tanaka, S. Hayashida, K. Imamura, H. Morishita, and Y. Koyanagi, “A study on miniaturization of a handset antenna utilizing magnetic materials,” in *Proc. Joint Conf. 10th Asia-Pacific Conf. Communications and Proc. 5th Int. Symp. Multi-Dim. Mobile Communications*, vol. 2, Aug. 2004, pp. 665–669.

[48] K.-S. Min and T. V. Hong, “Miniaturization of antenna using magneto-dielectric materials,” in *Proc. Asia-Pacific Conf. Communications (APCC)*, Busan, Korea, Aug. 2006, pp. 1–5.

[49] Y. Deng and Q.-X. Chu, “Comb-shaped antenna on magneto-dielectric substrate for DVB-H reception,” in *Proc. Int. Conf. Microw. Millimeter Wave Tech. (ICMMT ’07)*, Guilin, China, Apr. 2007, pp. 1–3.

[50] N. Sun, J. Wang, A. Daigle, C. Pettiford, H. Mosallaei, and C. Vittoria, “Electronically tunable magnetic patch antennas with metal magnetic films,” *Electron. Lett.*, vol. 8, no. 8, pp. 434–436, Apr. 2007.

[51] F. He, Z. Wu, and J. C. Modro, “Organic magnetic material measurement and its application on antenna,” in *Proc. IEEE Int. Workshop Antenna Tech. (iWAT)*, Chiba, Japan, 4-6 Mar. 2008, pp. 143–146.

[52] G. Yang, A. Daigle, J. W. Wang, N. X. Sun, and K. Naishadham, “Tunable miniaturized patch antennas at 2.1 GHz using self-biased magnetic films,” in *Proc. Int. Workshop Antenna Tech. (iWAT)*, 2008, pp. 115–118.

[53] G. Yang, A. Daigle, M. Liu, O. Obi, S. Stoute, K. Naishadham, and N. Sun, “Planar circular loop antennas with self-biased magnetic film loading,” *Electron. Lett.*, vol. 44, no. 5, pp. 332–333, Feb. 2008.

[54] R. Petrov, A. Tatarenko, S. Pandey, G. Srinivasan, J. Mantese, and R. Azadegan, “Miniature antenna based on magnetoelectric composites,” *Electron. Lett.*, vol. 44, no. 8, pp. 506–507, Apr. 2008.

[55] R. V. Petrov, A. S. Tatarenko, G. Srinivasan, and J. V. Mantese, “Antenna miniaturization with ferrite ferroelectric composites,” *Microwave Opt. Technol. Lett.*, vol. 50, no. 12, pp. 3154–3157, Dec. 2008.

[56] Y. S. Shin and S. O. Park, “A chip antenna with magneto-dielectric material,” in *Proc. IEEE Antennas Propag. Int. Symp.*, New Orleans, LA, 2008.

[57] S. Bae, Y. K. Hong, and A. Lyle, “Effect of Ni-Zn ferrite on bandwidth and radiation efficiency of embedded antenna for mobile phone,” *J. Appl. Phys*, vol. 103, pp. 07E929–3, 2008.

[58] F. Grange, K. Garello, E. Benevent, S. Bories, B. Viala, C. Delaveaud, and K. Mahdjoubi, "Investigation of magneto-dielectric thin films as substrates for patch antennas," in *Proc. 3rd European Conf. Antennas Propag. (EuCAP)*, Berlin, Germany, 23-27 Mar. 2009, pp. 1909–1913.

[59] G. M. Yang, X. Xing, A. Daigle, M. Liu, O. Obi, S. Stoute, K. Naishadham, and N. X. Sun, "Tunable miniaturized patch antennas with self-biased multilayer magnetic films," *IEEE Trans. Antennas Propag.*, vol. 57, no. 7, pp. 2190–2193, Jul. 2009.

[60] Y. Cheon, J. Lee, and J. Lee, "Quad-band monopole antenna including LTE 700 MHz with magneto-dielectric material," *IEEE Antennas Wireless Propag. Lett.*, 2012, early access.

[61] J. Lee, J. Heo, J. Lee, and Y. Han, "Design of small antennas for mobile handsets using magneto-dielectric material," *IEEE Trans. Antennas Propag.*, vol. 60, no. 4, pp. 2080–2084, Apr. 2012.

[62] P. Ikonen and S. Tretyakov, "On the advantages of magnetic materials in microstrip antenna miniaturization," *Microwave Opt. Technol. Lett.*, vol. 50, no. 12, pp. 3131–3134, Dec. 2008.

[63] S. Tretyakov, *Analytical Modeling in Applied Electromagnetics*. Norwood, MA: Artech House, 2003.

[64] O. S. Kim, "Electric dipole antennas with magnetic-coated PEC cores: Reaching the Chu lower bound on Q," *IEEE Trans. Antennas Propag.*, vol. 60, no. 3, pp. 1616–1619, Mar. 2012.

[65] T. V. Hansen, O. S. Kim, and O. Breinbjerg, "Stored energy and quality factor of spherical wave functions – in relation to spherical antennas with material cores," *IEEE Trans. Antennas Propag.*, vol. 60, no. 3, pp. 1281–1290, Mar. 2012.

[66] J. Ollikainen, "Design and implementation techniques of wideband mobile communications antennas," Doctoral thesis, Helsinki University of Technology, 2004. [Online]. Available: http://lib.tkk.fi/Diss/2004/isbn9512273810/

[67] P. Vainikainen, J. Ollikainen, O. Kivekäs, and I. Kelander, "Resonator-based analysis of the combination of mobile handset antenna and chassis," *IEEE Trans. Antennas Propag.*, vol. 50, no. 10, pp. 1433–1444, Oct. 2002.

[68] J. Villanen, J. Ollikainen, O. Kivekäs, and P. Vainikainen, "Coupling element based mobile terminal antenna structures," *IEEE Trans. Antennas Propag.*, vol. 54, no. 7, pp. 2142–2153, Jul. 2006.

[69] J. Holopainen, "Compact UHF-band antennas for mobile terminals: Focus on modelling, implementation, and user interaction," Doctoral thesis, Aalto University, 2011. [Online]. Available: http://lib.tkk.fi/Diss/2011/isbn9789526040868/

[70] M. Hirvonen, A. Hujanen, J. Holmberg, and J. C.-E. Sten, "Bandwidth limitations of dipoles matched with non-Foster impedances," in *Proc. Second European Conf. Antennas Propag. (EuCAP)*, Edinburgh, UK, 11-16 Nov. 2007.

[71] S. E. Sussman-Fort and R. M. Rudish, "Non-Foster impedance matching of electrically-small antennas," *IEEE Trans. Antennas Propag.*, vol. 57, no. 8, pp. 2230–2241, Aug. 2009.

[72] K.-S. Song and R. G. Rojas, "Electrically small wire monopole antenna with non-Foster impedance element," in *Proc. Fourth European Conf. Antennas Propag. (EuCAP)*, Barcelona, Spain, 12-16 Apr. 2010.

[73] P. Jin and R. W. Ziolkowski, "Broadband, efficient, electrically small metamaterial-inspired antennas facilitated by active near-field resonant parasitic elements," *IEEE Trans. Antennas Propag.*, vol. 58, no. 2, pp. 318–327, Feb. 2010.

[74] H. Mirzaei and G. V. Eleftheriades, "A wideband metamaterial-inspired compact antenna using embedded non-Foster matching," in *Proc. IEEE Int. Antennas Propag. Symp.*, Spokane, WA, 3-8 Jul. 2011, pp. 1950–1953.

[75] P. Ikonen, "Electrically small metamaterial-based antennas – have we seen any real practical benefits?" in *Proc. 3rd European Conf. Antennas Propag. (EuCAP)*, Berlin, Germany, 23-27 Mar. 2009, pp. 866–869.

[76] D. Sievenpiper, L. Zhang, R. Broas, N. Alexopolous, and E. Yablonovitch, "High-impedance electromagnetic surfaces with a forbidden frequency band," *IEEE Trans. Microw. Theory Tech.*, vol. 47, no. 11, pp. 2059–2074, Nov. 1999.

[77] S. A. Tretyakov and C. R. Simovski, "Wire antennas near artificial impedance surfaces," *Microwave Opt. Technol. Lett.*, vol. 27, no. 1, pp. 46–50, Oct. 2000.

[78] R. C. Hansen, "Effects of a high-impedance screen on a dipole antenna," *IEEE Antennas Wireless Propag. Lett.*, vol. 1, pp. 46–49, 2002.

[79] O. Luukkonen, "Artificial impedance surfaces," Doctoral thesis, Helsinki University of Technology, 2009. [Online]. Available: http://lib.tkk.fi/Diss/2009/isbn9789522482525/

[80] F. Yang and Y. Rahmat-Samii, "Reflection phase characterizations of the EBG ground plane for low profile wire antenna applications," *IEEE Trans. Antennas Propag.*, vol. 51, no. 10, pp. 2691–2703, Oct. 2003.

[81] O. Luukkonen, C. Simovski, G. Granet, G. Goussetis, D. Lioubtchenko, A. V. Räisänen, and S. A. Tretyakov, "Simple and accurate analytical model of planar grids and high-impedance surfaces comprising metal strips or patches," *IEEE Trans. Antennas Propag.*, vol. 56, no. 6, pp. 1624–1632, Jun. 2008.

[82] O. Luukkonen, M. G. Silveirinha, A. B. Yakovlev, C. R. Simovski, I. S. Nefedov, and S. A. Tretyakov, "Effects of spatial dispersion on reflection from mushroom-type artificial impedance surfaces," *IEEE Trans. Microw. Theory Tech.*, vol. 57, no. 11, pp. 2692–2699, Nov. 2009.

[83] A. B. Yakovlev, M. G. Silveirinha, O. Luukkonen, C. R. Simovski, I. S. Nefedov, and S. A. Tretyakov, "Characterization of surface-wave and leaky-wave propagation on wire-medium slabs and mushroom structures based on local and nonlocal homogenization models," *IEEE Trans. Microw. Theory Tech.*, vol. 57, no. 11, pp. 2700–2714, Nov. 2009.

[84] F. Costa, O. Luukkonen, C. R. Simovski, A. Monorchio, S. A. Tretyakov, and P. M. de Maagt, "TE surface wave resonances on high-impedance surface based antennas: Analysis and modeling," *IEEE Trans. Antennas Propag.*, vol. 59, no. 10, pp. 3588–3596, Oct. 2011.

[85] C. Allen, K. Leong, and T. Itoh, "Design of a balanced 2D composite right-/left-handed transmission line type continuous scanning leaky-wave antenna," *IET Microw. Antennas Propag.*, vol. 1, no. 3, pp. 746–750, Jun. 2007.

[86] A. Karilainen, "Thin-sheet antennas based on networks of loaded transmission lines," Master's thesis, Helsinki University of Technology, 2008. [Online]. Available: http://lib.tkk.fi/Dipl/2008/urn012125.pdf

[87] T. Zhao, T. Zhao, D. Jackson, J. Williams, and A. Oliner, "General formulas for 2-D leaky-wave antennas," *IEEE Trans. Antennas Propag.*, vol. 53, no. 11, pp. 3525–3533, Nov. 2005.

[88] F. Costa, A. Monorchio, S. Talarico, and F. M. Valeri, "An active high-impedance surface for low-profile tunable and steerable antennas," *IEEE Antennas Wireless Propag. Lett.*, vol. 7, pp. 676–680, 2008.

[89] F. Costa, A. Monorchio, and G. Manara, "Low-profile tunable and steerable Fabry-Perot antenna for software defined radio applications," in *Proc. IEEE Antennas Propag. Soc. Int. Symp.*, Toronto, ON, 11-17 Jul. 2010.

[90] C. Guclu, J. Sloan, S. Pan, and F. Capolino, "High impedance surface as an antenna without a dipole on top," in *Proc. IEEE Antennas Propag. Soc. Int. Symp.*, 2011, pp. 1028–1031.

[91] ——, "Direct use of the high impedance surface as an antenna without dipole on top," *IEEE Antennas Wireless Propag. Lett.*, vol. 10, pp. 1536–1539, 2011.

[92] O. Luukkonen, P. Alitalo, F. Costa, C. Simovski, A. Monorchio, and S. Tretyakov, "Experimental verification of the suppression of spatial dispersion in artificial plasma," *Appl. Phys. Lett.*, vol. 96, p. 081501, 2010.

[93] M. A. Antoniades and G. V. Eleftheriades, "A folded-monopole model for electrically small NRI-TL metamaterial antennas," *IEEE Antennas Wireless Propag. Lett.*, vol. 7, pp. 425–428, 2008.

[94] J. Clerk Maxwell, *A Treatise on Electricity and Magnetism*. Oxford, UK: Clarendon, 1873, vol. 2.

[95] H. A. Wheeler, "Fundamental limitations of small antennas," *Proc. IRE*, vol. 35, no. 12, pp. 1479–1484, Dec. 1947.

[96] ——, "A helical antenna for circular polarization," *Proc. IRE*, vol. 35, no. 12, pp. 1484–1488, Dec. 1947.

[97] J. D. Kraus, "Helixal beam antenna," *Electronics*, vol. 20, pp. 109–111, Apr. 1947.

[98] ——, "The helical antenna," *Proc. IRE*, vol. 37, no. 3, pp. 263–272, Mar. 1949.

[99] D. L. Jaggard, A. R. Mickelson, and C. H. Papas, "On electromagnetic waves in chiral media," *Appl. Phys. A*, vol. 18, no. 2, pp. 211–216, 1979.

[100] C. T. Tai, *Dyadic Green's Functions in Electromagnetic Theory*. Scranton, PA: Intext, 1971.

[101] I. V. Lindell, A. Sihvola, P. Ylä-Oijala, and H. Wallén, "Zero backscattering from self-dual objects of finite size," *IEEE Trans. Antennas Propag.*, vol. 57, no. 9, pp. 2725–2731, Sep. 2009.

[102] R. B. Green, "Scattering from conjugate-matched antennas," *IEEE Trans. Antennas Propag.*, vol. 14, no. 1, pp. 17–21, Jan. 1966.

[103] J. McLean and G. Crook, "$P \times M$ antennas for immunity testing and other field generation applications," in *Proc. IEEE Int. Symp. Electromagn. Comp.*, vol. 2, Seattle, WA, 2-6 Aug. 1999, pp. 624–628.

[104] J. McLean and R. Sutton, *Ultra-Wideband, Short-Pulse Electromagnetics*. New York, NY: Springer, 2007, ch. Practical Realization of PxM Antennas for High-Power, Broadband Applications, pp. 267–275.

[105] M. J. Underhill and M. J. Blewett, "Undirectional tuned loop antennas using combined loop and dipole," in *Proc. Eighth Int. Conf. Radio Systems Techniq.*, Guildford, UK, 10-13 Jul. 2000, pp. 37–41.

[106] P. Jin and R. W. Ziolkowski, "Metamaterial-inspired, electrically small Huygens sources," *IEEE Antennas Wireless Propag. Lett.*, vol. 9, pp. 501–505, 2010.

[107] A. Chlavin, "A new antenna feed having equal E- and H-plane patterns," *IRE Trans. Antennas Propag.*, vol. 2, no. 3, pp. 113–119, Jul. 1954.

[108] A. Clavin, D. Huebner, and F. Kilburg, "An improved element for use in array antennas," *IEEE Trans. Antennas Propag.*, vol. 22, no. 4, pp. 521–526, Jul. 1974.

[109] D. M. Pozar, "New results for minimum Q, maximum gain, and polarization properties of electrically small arbitrary antennas," in *Proc. 3rd European Conf. Antennas Propag. (EuCAP)*, Berlin, Germany, 23-27 Mar. 2009, pp. 1993–1996.

[110] K. M. Mak and K. M. Luk, "A circularly polarized antenna with wide axial ratio beamwidth," *IEEE Trans. Antennas Propag.*, vol. 57, no. 10, pp. 3309–3312, Oct. 2009.

[111] P. Jin and R. W. Ziolkowski, "High-directivity, electrically small, low-profile near-field resonant parasitic antennas," *IEEE Antennas Wireless Propag. Lett.*, vol. 11, pp. 305–309, 2012.

[112] D.-H. Kwon, "On the radiation Q and the gain of crossed electric and magnetic dipole moments," *IEEE Trans. Antennas Propag.*, vol. 53, no. 5, pp. 1681–1687, May 2005.

[113] D. M. Pozar, "Polarization of maximum gain antennas," *IEEE Trans. Antennas Propag.*, vol. 55, no. 7, pp. 2113–2115, Jul. 2007.

[114] D.-H. Kwon, "Radiation Q and gain of TM and TE sources in phase-delayed rotated configurations," *IEEE Trans. Antennas Propag.*, vol. 56, no. 8, pp. 2783–2786, Aug. 2008.

[115] D.-H. Kwon and D. M. Pozar, "Optimal characteristics of an arbitrary receive antenna," *IEEE Trans. Antennas Propag.*, vol. 57, no. 12, pp. 3720–3727, Dec. 2009.

[116] C. R. Simovski, S. A. Tretyakov, A. A. Sochava, B. Sauviac, F. Mariotte, and T. G. Kharina, "Antenna model for conductive omega particles," *J. Electrom. Waves App.*, vol. 11, no. 11, pp. 1509–1530, 1997.

[117] S. A. Tretyakov, F. Mariotte, C. R. Simovski, T. G. Kharina, and J. P. Heliot, "Analytical antenna model for chiral scatterers: comparison with numerical and experimental data," *IEEE Trans. Antennas Propag.*, vol. 44, no. 7, pp. 1006–1014, Jul. 1996.

[118] J. B. Andersen and A. Frandsen, "Absorption efficiency of receiving antennas," *IEEE Trans. Antennas Propag.*, vol. 53, no. 9, pp. 2843–289, Sep. 2005.

[119] M. Asghar, I. Hakala, J. Jantunen, H. Kettunen, M. Pitkonen, J. Qi, G. Statkute, A. Varpula, I. V. Semchenko, S. A. Khakhomov, R. Gonzalo, E. Ozbay, V. Podlozny, A. Sihvola, S. Tretyakov, and H. Wallén, "Electromagnetic cloaking with a mixture of spiral inclusions." in *Proc. Metamaterials*, Rome, Italy, 22-26 Oct. 2007.

[120] E. Saenz, I. Semchenko, S. Khakhomov, K. Guven, R. Gonzalo, E. Ozbay, and S. Treatyakov, "Modeling of spirals with equal dielectric, magnetic, and chiral susceptabilites," *Electromagnetics*, vol. 28, pp. 476–493, 2008.

[121] A. Alù and N. Engheta, "Cloaking a sensor," *Phys. Rev. Lett.*, vol. 102, p. 233901, 2009.

[122] ——, "Cloaking a receiving antenna or a sensor with plasmonic metamaterials," *Metamaterials*, vol. 4, pp. 153–159, 2010.

[123] J. J. Bowman, T. B. A. Senior, and P. L. E. Uslenghi, Eds., *Electromagnetic and Acoustic Scattering by Simple Shapes*. Amsterdam, The Netherlands: North-Holland Publishing Company, 1969.

[124] S. A. Tretyakov, S. Maslovski, and P. A. Belov, "An analytical model of metamaterials based on loaded wire dipoles," *IEEE Trans. Antennas Propag.*, vol. 51, no. 10, pp. 2652–2658, Oct. 2003.

[125] A. Alù and S. Maslovski, "Power relations and a consistent analytical model for receiving wire antennas," *IEEE Trans. Antennas Propag.*, vol. 58, no. 5, pp. 1436–1448, May 2010.

[126] A. O. Karilainen and S. A. Tretyakov, "Isotropic chiral objects with zero backscattering," *IEEE Trans. Antennas Propag.*, 2012, early access.

[127] T. Niemi, "Polarization transformations in bianisotropic arrays," Master's thesis, Aalto University, March 2012. [Online]. Available: http://lib.tkk.fi/Dipl/2012/urn100588.pdf

Errata

Publication II

In Section 3, p. 497, the thickness of the Mylar substrate is 12 μm, not 0.07 μm.

Electric and magnetic fields have been known to be a manifestation of the same physical phenomenon for almost two hundred years, but some aspects of electromagnetism are not in balance in nature around us. We are faced with restrictions due to lack of real magnetic charges, currents, and conductors. However, it has turned out that virtual magnetic currents and conductors and magnetic materials can be engineered and used in a variety of applications, antennas being one amongst them. This doctoral thesis focuses on magnetic materials and artificially created magnetic responses in antenna applications. The thesis is divided into three research problems concerning antennas in which the magnetic part of Maxwell's equations plays a key role. The common goal in each of these parts is to improve the properties of the antennas in question or to conjure new types of antennas.

Aalto-DD 93/2012

ISBN 978-952-60-4704-1
ISBN 978-952-60-4705-8 (pdf)
ISSN-L 1799-4934
ISSN 1799-4934
ISSN 1799-4942 (pdf)

Aalto University
School of Electrical Engineering
Department of Radio Science and Engineering
www.aalto.fi

BUSINESS + ECONOMY

ART + DESIGN + ARCHITECTURE

SCIENCE + TECHNOLOGY

CROSSOVER

DOCTORAL DISSERTATIONS